คุณลักษณะและสมบัติในการเร่งปฏิกิริยาของตัวเร่งปฏิกิริยาแพลทินัมบนไทเทเนียที่ปรับปรุงด้วยซิงค์และแลนทานัมในปฏิกิริยาไฮโดรจิเนชันแบบเลือกเกิดของ 3-ไนโตรสไตรีน

นายอาณัติ แซ่อ้วง

วิทยานิพนธ์นี้เป็นส่วนหนึ่งของการศึกษาตามหลักสูตรปริญญาวิศวกรรมศาสตรมหาบัณฑิต
สาขาวิชาวิศวกรรมเคมี ภาควิชาวิศวกรรมเคมี
คณะวิศวกรรมศาสตร์ จุฬาลงกรณ์มหาวิทยาลัย
ปีการศึกษา 2558

CHARACTERISTICS AND CATALYTIC PROPERTIES OF Pt CATALYSTS SUPPORTED ON Zn AND La-MODIFIED TiO_2 IN SELECTIVE HYDROGENATION OF 3-NITROSTYRENE

Mr. Arnut Saeaung

A Thesis Submitted in Partial Fulfillment of the Requirements
for the Degree of Master of Engineering Program in Chemical Engineering
Department of Chemical Engineering
Faculty of Engineering
Chulalongkorn University
Academic Year 2015

Thesis Title	CHARACTERISTICS AND CATALYTIC PROPERTIES OF Pt CATALYSTS SUPPORTED ON Zn AND La-MODIFIED TiO_2 IN SELECTIVE HYDROGENATION OF 3-NITROSTYRENE
By	Mr. Arnut Saeaung
Field of Study	Chemical Engineering
Thesis Advisor	Associate Professor Joongjai Panpranot, Ph.D.

Accepted by the Faculty of Engineering, Chulalongkorn University in Partial Fulfillment of the Requirements for the Master's Degree

.....Dean of the Faculty of Engineering

(Associate Professor Supot Teachavorasinskun, D.Eng.)

THESIS COMMITTEE

.....Chairman

(Professor Suttichai Assabumrungrat, Ph.D.)

.....Thesis Advisor

(Associate Professor Joongjai Panpranot, Ph.D.)

.....Examiner

(Palang Bumroongsakulsawat, Ph.D.)

.....External Examiner

(Assistant Professor Okorn Mekasuwandumrong, D.Eng.)

อาณัติ แซ่อ้วง : คุณลักษณะและสมบัติในการเร่งปฏิกิริยาของตัวเร่งปฏิกิริยาแพลทินัมบนไทเทเนียที่ปรับปรุงด้วยซิงค์และแลนทานัมในปฏิกิริยาไฮโดรจิเนชันแบบเลือกเกิดของ 3-ไนโตรสไตรีน (CHARACTERISTICS AND CATALYTIC PROPERTIES OF Pt CATALYSTS SUPPORTED ON Zn AND La-MODIFIED TiO_2 IN SELECTIVE HYDROGENATION OF 3-NITROSTYRENE) อ.ที่ปรึกษาวิทยานิพนธ์หลัก: รศ. ดร.จูงใจ ปั้นประณต, 75 หน้า.

ศึกษาผลของการปรับปรุงไทเทเนียด้วยซิงค์และแลนทานัมต่อสมบัติในการเร่งปฏิกิริยาของตัวเร่งปฏิกริยาแพลทินัมบนไทเทเนียในปฏิกิริยาไฮโดรจิเนชันแบบเลือกเกิดของสามไนโตรสไตรีน โดยเตรียมไทเทเนียด้วยวิธีโซลโวเทอร์มอลที่อุณหภูมิ 320 องศาเซลเซียส และเติมซิงค์หรือแลนทานัม และนำไปใช้เป็นตัวรองรับในการเตรียมตัวเร่งปฏิกิริยาแพลทินัม รีดิวซ์ตัวเร่งปฏิกิริยาที่อุณหภูมิต่ำ (200 องศาเซลเซียส) และอุณหภูมิสูง (500 องศาเซลเซียส) ก่อนการทดสอบในปฏิกิริยาไฮโดรจิเนชันแบบเลือกเกิดของไนโตรสไตรีนในเครื่องปฏิกรณ์แบบกะ ภายใต้ความดันไฮโดรเจน 2 เมกะปาสคาล และอุณหภูมิ 40 องศาเซลเซียส วิเคราะห์คุณลักษณะของตัวเร่งปฏิกิริยาด้วยเทคนิค การดูดซับทางกายภาพด้วยแก๊สไนโตรเจน การกระเจิงรังสีเอ็กซ์ รีดักชันของไฮโดรเจนด้วยการโปรแกรมอุณหภูมิ การดูดซับทางเคมีด้วยแก๊สคาร์บอนมอนอกไซด์ กล้องจุลทรรศน์อิเล็กตรอนแบบส่องผ่าน เอ็กซเรย์โฟโตอิเล็กตรอนสเปกโตรสโกปีและอินฟราเรดสเปกโตรสโกปีของการดูดซับด้วยแก๊สคาร์บอนมอนอกไซด์ การเติมซิงค์เพื่อปรับปรุงไทเทเนียช่วยเพิ่มค่าการเปลี่ยนไปของสามไนโตรสไตรีนร้อยละ 64 เมื่อเปรียบเทียบกับไทเทเนียที่ไม่ได้ปรับปรุงที่ร้อยละ 44 ที่อุณหภูมิรีดักชันสูงซึ่งสอดคล้องกับผลของเทคนิคการดูดซับทางกายภาพด้วยแก๊สไนโตรเจนและการดูดซับทางเคมีด้วยแก๊สคาร์บอนมอนอกไซด์ ตัวเร่งปฏิกริยาบนไทเทเนียที่ปรับปรุงด้วยซิงค์มีพื้นที่ผิวและปริมาณของแหล่งกัมมันต์ที่มากกว่า (การกระจายตัวของโลหะสูงกว่า) นอกจากนี้ตัวเร่งปฏิกริยาบนไทเทเนียที่ปรับปรุงด้วยซิงค์ยังแสดงค่าการเลือกเกิดของไวนิลอะนิลีนที่สูง ตรงข้ามกับตัวเร่งปฏิกริยาบนไทเทเนียที่ปรับปรุงด้วยแลนทานัมที่ให้ค่าร้อยละของไวนิลอะนิลีนที่ต่ำกว่าตัวเร่งปฏิกริยาที่ไม่ถูกปรับปรุงเพราะว่าปริมาณของแหล่งกัมมันต์ที่น้อยกว่าดังแสดงโดยผลของการดูดซับทางเคมีด้วยแก๊สคาร์บอนมอนอกไซด์

ภาควิชา วิศวกรรมเคมี ลายมือชื่อนิสิต .....

สาขาวิชา วิศวกรรมเคมี ลายมือชื่อ อ.ที่ปรึกษาหลัก .....

ปีการศึกษา 2558

5770364021 : MAJOR CHEMICAL ENGINEERING

KEYWORDS: PT/TIO2 / LIQUID-PHASE SELECTIVE HYDROGENATION / 3-NITROSTYRENE / ZN-MODIFIED / LA-MODIFIED

ARNUT SAEAUNG: CHARACTERISTICS AND CATALYTIC PROPERTIES OF Pt CATALYSTS SUPPORTED ON Zn AND La-MODIFIED TiO_2 IN SELECTIVE HYDROGENATION OF 3-NITROSTYRENE. ADVISOR: ASSOC. PROF. JOONGJAI PANPRANOT, Ph.D., 75 pp.

The effect of Zn and La modified TiO_2 on the catalytic performances of Pt/TiO_2 was studied in the liquid-phase selective hydrogenation of 3-nitrostyrene (NS). Titanium dioxide (TiO_2) was prepared by the solvothermal method at 320 ℃ with and without Zn and La modification and used as a support for preparation of TiO_2 supported Pt catalysts. The catalysts were reduced at low (200 ℃) and high (500℃) reduction temperatures before the reaction tests. The hydrogenation of NS was carried out batchwise at H_2 pressure 2 MPa and 40 ℃. The catalysts were characterized by N_2-physisorption, X-ray diffraction (XRD), H_2-temperature program reduction (H_2-TPR), CO chemisorption, transmission electron microscopy (TEM), X-ray photoelectron spectroscopy (XPS) and FT-IR analysis of adsorbed CO (CO-IR). The use of Zn-modified TiO_2 provided higher NS conversion (64%) compared to the unmodified one (44%) at high reduction temperature. According to the N_2-physisorption and CO chemisorption results, the Pt/Zn-modified TiO_2 had greater BET surface areas compared to the Pt/TiO_2 and higher amount of Pt active sites (higher Pt dispersion). The Zn-modified TiO_2 supported Pt catalysts also exhibited high VA selectivity. In contrast, the Pt/La-modified TiO_2 provided the lower vinylaniline yield compared to the unmodified catalysts because of lower amount of active sites as determined by the CO-chemisorption results.

Department: Chemical Engineering Student's Signature .....

Field of Study: Chemical Engineering Advisor's Signature .....

Academic Year: 2015

ACKNOWLEDGEMENTS

The author would like to express his thankfulness and appreciation to his advisor, Associate Professor Joongjai Panpranot, for her valuable suggestions, encouragement and useful discussion throughout this research. In addition, the author would also be grateful to Professor Sutthichai Assabumrungrat as the chairman, Dr. Palang Bumroongsakulsawat and Assistant Professor Okorn Mekasuwandumrong as the member of Thesis committee.

Moreover, the author would like to express his gratitude to his parents, all of his friends and the members of the Center of Excellence on Catalysis and Catalytic Reaction Engineering, Department of Chemical Engineering, Faculty of Engineering, Chulalongkorn University.

Finally, the author kindly thanks the Thailand Research Fund (TRF), as well as the Graduate School of Chulalongkorn University for their financial supports.

CONTENTS

Page

Page

Page

Page

LIST OF TABLES

Page

Page

LIST OF FIGURES

Page

Page

CHAPTER I
INTRODUCTION

1.1 Motivation

Nitrogen is useful in a variety of chemicals such as polymers, fertilizers, dyes, or biologically active compounds. Nitrogen is often integrated into these chemicals from HNO_3 by nitration reaction at the earliest steps and the nitro compounds as products are the building blocks in organic synthesis. The nitration reaction is a route to obtain nitroaromatic compounds and short nitroalkanes because the high selectivity towards the mononitrated products following standard industrial protocols [1]. Nitration of aromatic compounds is a fundamental reaction of great industrial importance and the nitro aromatic compounds are key organic intermediated. The nitrating reagent such as a mixture of sulfuric acid with concentrated fuming nitric acid has always been used for nitration of benzene, alkyl benzene and less reactive aromatic compounds [2]. The nitration of styrene has been used to produce nitrostyrene. The interest in hydrogenation of nitro compounds has increased in the past decade. Nitroarenes hydrogenation is an important chemoselective reaction for the production of intermediates used in polymer, pharmaceuticals herbicides, and other fine chemicals industry [3, 4]. Nitroarenes consist of nitro groups with other reducible groups. The challenge is how to hydrogenate nitro groups while avoiding to cleavage other reducible groups (the latter must be retained to preserve products with high synthetic value) [5, 6]. Moreover, getting both of high selectivity and high activity are difficult because of increasing the activity always cause the selectivity decreased. Nowadays, the commercial production of nitroarenes containing these reducible groups is obtained through non-catalytic methods using a stoichiometric amount of iron, tin, or other reducing reagents which produces a large amount of solid wastes and brings about serious environmental issues [7]. Heterogeneous catalysts were developed for solving these problems. Noble metals such as Pt and Ru have been used in chemoselecive hydrogenation due to their high activities [8, 9]. However, noble

metals are not chemoselective but can be modified to improve the selectivities while maintaining the activities. There were many attempts to overcome these problems.

TiO_2 is a reducible metal oxide which provides a strong metal-support interaction (SMSI) with noble metals compared to the other metal oxides[10]. Corma et al.[9]studied the transforming of non-selective into chemoselective metal catalysts for the hydrogenation of substituted nitroaromatics. They concluded that reduction catalyst at high temperature can promote the selectivity towards nitro group due to the decoration of Pt crystal surfaces, decreasing the amount of Pt terraces sites. The terrace Pt sites were blocked by TiO_x species due to strong metal-support interaction (SMSI) at high reduction temperature and consequently increasing the amount of Pt-TiO_x sites. Moreover, TiO_2 can avoid the accumulation of reaction intermediates.

A simply method to modify the properties of TiO_2 such as crystallite size, surface area, metal dispersion and metal-support interaction is by addition of another metal element to the TiO_2 support. Comsup, N. [11] investigated the influence of Si-modified TiO_2 on the activity of Ag/TiO_2 in CO oxidation. Si-modified TiO_2 were prepared by solvothermal method. According to the FT-IR results, when adding Si into TiO_2 support the agglomeration of TiO_2 crystallites were inhibited, causing both surface area and metal dispersion increased.

Solvothermal is a synthesis method of nanocrystalline particles. The shape or morphologies of particles can be easily controlled by adjusting the parameters such as temperature, pressure, type of solvent and etc.

In this research, TiO_2 was prepared by the solvothermal method with and without Zn and La modification and used as the supports for preparation of TiO_2 supported Pt catalysts for the selective hydrogenation of 3-nitrostyrene to vinylaniline.

1.2 Objective

To investigate the characteristics and performances of Zn and La modified TiO_2 supported Pt catalysts in the liquid phase selective hydrogenation of 3-nitrostyrene.

1.3 Research scope

1) Preparation of the TiO_2 supports, Zn and La-modified TiO_2 supports by using the solvothermal method.
2) Preparation of the Pt/TiO_2, Pt/Zn and La-modified TiO_2 by using the incipient wetness impregnation method with an aqueous solution of 0.5% wt $H_2PtCl_6 \cdot 6H_2O$.
3) Preparation of the Pt/TiO_2, Pt/Zn and La-modified TiO_2 by sequential-impregnation method and co-impregnation method with an aqueous solution of 0.5% wt $H_2PtCl_6 \cdot 6H_2O$.
4) Catalyst calcination in air at 450°C for 3 h and followed by reduction in H_2 flow at 200 °C and 500 °C.
5) Reaction study in the liquid-phase selective hydrogenation of 3-nitrostyrene to 3-vinylaniline by using the stirred batch reactor under H_2 pressure of 2 MPa and temperature of 40 °C.
6) Catalyst characterization using various techniques

    - X-ray diffraction (XRD)
    - N_2 physisorption
    - X-ray photoelectron spectroscopy (XPS)
    - CO-Pulse chemisorption
    - H_2 temperature program reduction
    - FT-IR analysis of adsorbed CO (CO-IR)

1.4 Research Methodology

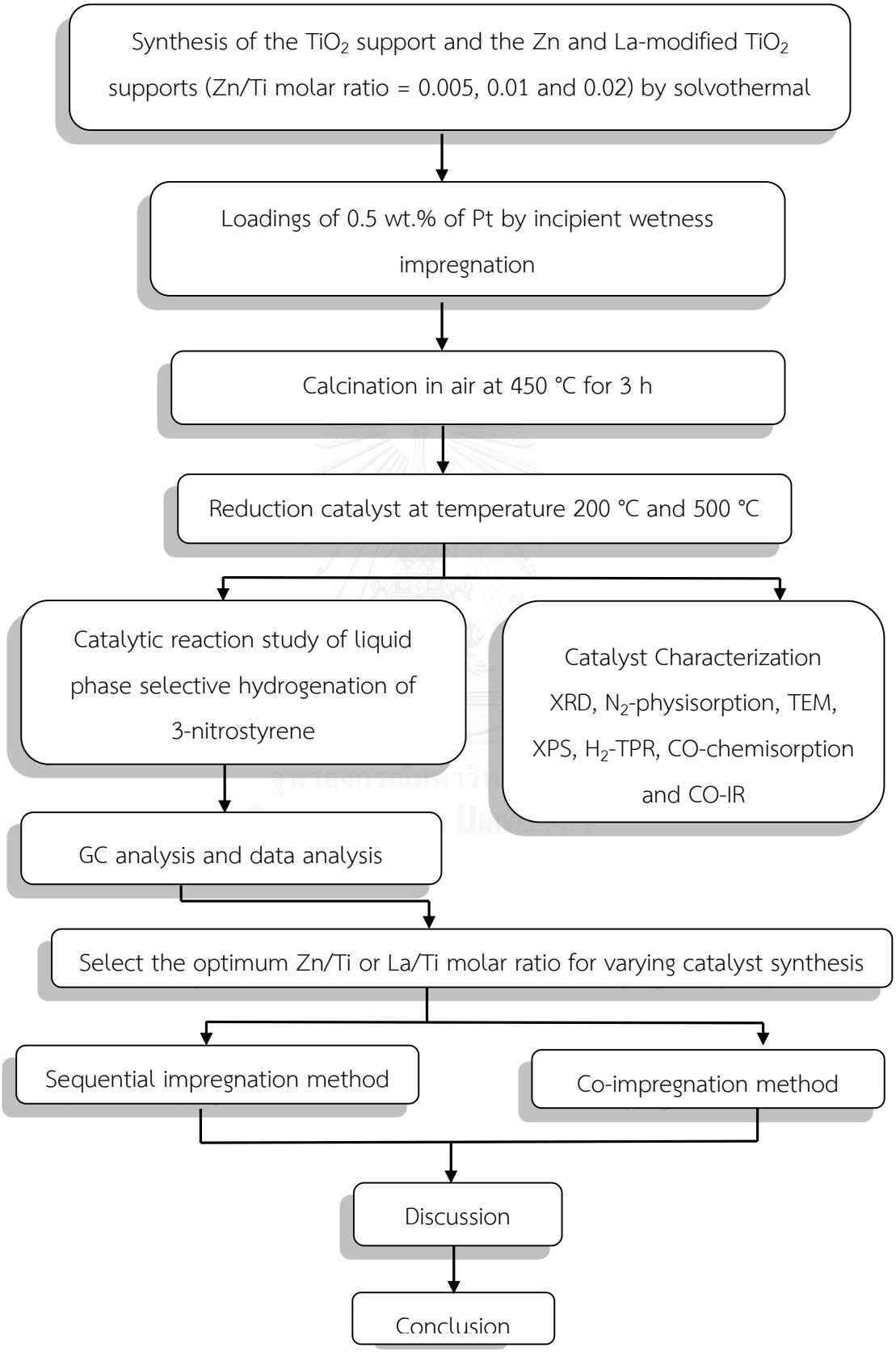

CHAPTER II
LITERATURE REVIEWS

This chapter provides the important details which related to catalyst properties, catalyst preparation, support modification, selective hydrogenation and effects of reduction temperature on catalytic performance. Moreover, the literatures which involved to this research were reviewed in this chapter as well.

2.1 Study on TiO_2 (Titanium dioxide) as support

TiO_2 has been widely utilized as a pigment and in sunscreens, paints, ointments, toothpaste and etc[12]. TiO_2 is one of the metal oxides which frequently be used as based catalyst support due to strong interaction with metal compared with the other metal oxides. This interaction affects the metal dispersion which influenced on catalytic activity and selectivity of the metal heterogeneous catalyst [13, 14]. There are three commonly crystalline structures of TiO_2: anatase, rutile and brooktile. Among the TiO_2 modifications, anatase is frequently utilized as a catalyst support for metal heterogeneous catalyst due to its high specific surface area and strong interaction with metal nanoparticles. There are only a few studies reporting a rutile catalyst support which resulted in higher catalytic activity compared to anatase such as the oxidation of toluene, xylene, and benzene over rutile supported Cu catalyst [15].

Ananthan, S.A., *et al*. (2011) [16] studied the TiO_2 supported Pt and Ru nanocatalysts for selective hydrogenation of citral. The catalysts were prepared by impregnation method and were reduced at two different temperatures at 375 °C and 575 °C. The reduction temperature caused the occurrence of TiO_x or presence of partially reduced species in TiO_2 which promoted the hydrogenation of C=O bond. The occurrence of unsaturated Ti cation strengthened the interaction of the C=O bond with the catalyst resulting high selectivity of C=O bond. The catalyst results shows 95% conversion and 68% selectivity of unsaturated alcohol which obtained from 1.5 %wt. Pt/TiO_2 at high reduction temperature.

Yoshida, H., *et al*. (2015) [17] studied the effects of TiO_2 crystallite size on the activity of dispersed Pt catalysts in liquid-phase selective hydrogenation of 3-nitrostyrene, nitrobenzene, and styrene. The crystallite size improved the formation of Pt particles that were selective for nitro group more than vinyl group. The results demonstrated that smaller TiO_2 crystallite size is effective for the formation of a larger fraction of low coordinated Pt sites on the surface of dispersed Pt particles which provides high selectivity to vinylaniline.

2.2 Selective hydrogenation reaction

Hydrogenation reaction is a chemical reaction between H_2 molecules and another compounds or elements usually in the presence of catalysts such as Ni, Pt and Pd.

The hydrogenation of nitroarenes are important for industry in the last ten years that has interest in highly chemoselective catalysts [1]. Nitroarenes consist of one nitro group and the other reducible groups. For example, nitrochlorobenzne consist of one nitro group and one Cl atom. The performance of selective hydrogenation in the presence of sensitive groups such as C=C bond group or triple bond group has been focused. For liquid phase selective hydrogenation of 3-nitrostyrene, the H_2 molecules reacts with the only nitro group (NO_2-) to form 3-vinylaniline (3-VA) which is a desired product or reacts with the only C=C double bond group to form ethylnitrobenzene (3-ENB). Moreover, both of 3-vinylaniline and 3-ethylnitrobenzene can further be hydrogenated to form 3-ethylaniline (3-EA) concurrently which are shown in Figure 2.1

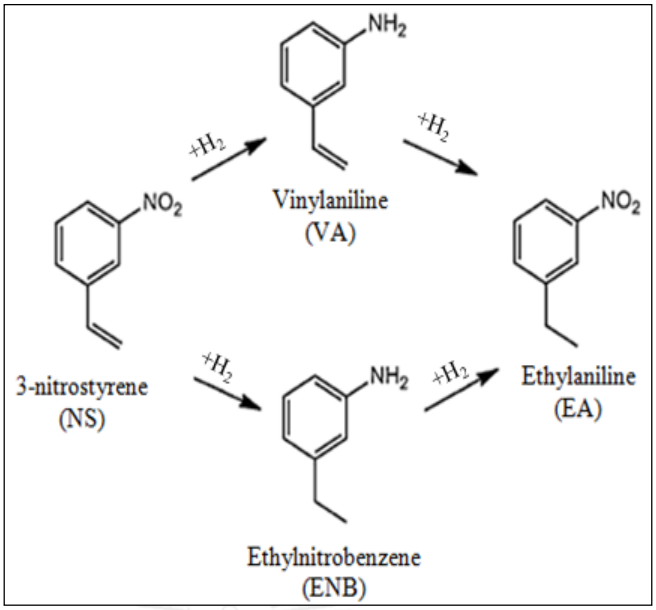

Figure 2.1 Reaction pathways in 3-nitrostyrene hydrogenation

Boronat, M., *et al.* (2007) [18] investigated a molecular mechanism for the chemoselective hydrogenation of substituted nitroaromatics with gold nanoparticles on TiO_2 catalysts. The gold nanoparticles on TiO_2 was highly chemoselective in hydrogenation of substituted nitroaromatics. The cooperation effect between Au and TiO_2 support allowed the preferential adsorption of nitro group which is not detected in Au/SiO_2 catalyst. From IR studies, both of nitro and olefinic groups weakly adsorbed on Au(111) and Au(001) and the stronger adsorption on low-coordinates atom of Au is unselective.

Shimizu, K., *et al.* (2009) [19] studied the effects of gold nanoparticles size and type of supports towards the activity of chemoselective hydrogenation of nitroaromatics. The catalysts such as Au/γ-Al_2O_3, Au/SiO_2, Au/montmorillonite, Au/MgO and Au/C were prepared by colloid deposition method. The gold catalysts showed the high selectivity towards the nitro groups of the substituted nitroaromatics. The acid-base sites of Al_2O_3 and the unsaturated Au atoms enhanced the H_2 dissociations to H^+/H^- pairs at metal-support interfaces. The H^+/H^- pairs which preferential transferred to the nitro group would enhance the high chemoselectivtiy.

Serna, P., *et al.* (2009) [20] designed the kinetic model for the chemoselective hydrogenation of nitroaromatic compound on Au/TiO_2 and $Pt\text{-}Au/TiO_2$. It was reported that the rate controlling step on Au/TiO2 is related to the H_2 dissociations on Au atoms on low coordination. In addition, the optimum content of Pt on bimetallic catalyst promoted the rate of H_2 dissociation which was almost one order of magnitude more active than monometallic Au/TiO_2. From catalyst results at 85 °C and 0.8 MPa , 1.5% wt. Au/TiO_2 performed the 3-NS conversion 97.8% and 3-VA 96.2 for 6 h while 0.2% wt. Pt/TiO_2 performed the 3-NS conversion 95.1% and 3-VA 69.7 for only 0.25 h. Compared to the 1.5 %wt. Au – 0.01%wt Pt $/TiO_2$, the bimetallic catalyst exhibited high activity than the monometallic 1.5% wt Au/TiO2 as conversion 94.5% and 3-VA selectivity 94.3% for 0.52 h at same reaction condition.

Yoshida, H., *et al.*(2011) [21] studied the nitrostyrene hydrogenation using Pt/TiO_2 catalysts in CO_2- dissolved ethanol and toluene at 50 °C. The effects of CO_2 pressure in both of non-polar solvent (toluene) and polar solvent (ethanol) on the total conversion and product selectivity were investigated. The CO_2 pressure decreased the rate of nitrostyrene hydrogenation in both of non-polar and polar solvent and changed the product selectivity only in non-polar solvent. The vinylaniline selectivity in toluene decreased with CO_2 pressure in contrast to ethylnitrobenzene selectivity due to the decreasing in the reactivity of the nitro group interacted with the CO_2 molecules.

Fujita, S.-i., *et al.* (2011) [22] studied the influenced of Pt loading (0.5 % wt. – 2 % wt.), reduction temperature and and effects of pressurized CO_2 towards the liquid phase selective 3-nitrostyrne hydrogenation. Increasing of Pt loading increased the crystallite size slightly and enhanced the catalytic activity as 2 % wt. Pt loading exhibited the 3-NS conversion at 97% compared to 0.5 % wt. Pt loading. Nonetheless, 2% wt. Pt loading catalyst showed the lower 3-vinylaniline (3-VA) selectivity about 34 % compared to 0.5 % wt. Pt loading about 75 %. According to CO-IR results, the adsorption band at 2065 cm^{-1} and at 2088 cm^{-1} related to the Pt edge sites and Pt terrace sites respectively. The results were revealed that the increasing of Pt loading provided the decreasing amount of unsaturated Pt at edge and corner sites caused the lower 3-VA selectivity consequently.

J.Beier, M., *et al.*(2012) [23] studied the tuning of chemoselective of hydrogenation of nitrostyrenes catalyzed by ionic liquid-supported platinum nanoparticles. Pt nanoparticles supported on various supports such as SiO_2, TiO_2, Al_2O_3 and CNTs were synthesized in ionic liquid. The influence of ionic liquid (acidic or basic) and types of support on catalytic behaviors were investigated. The NO_2 group were favorably hydrogenated to form 3-vinylaniline and reaction intermediate 3-(Nhydroxylamino)styrene under the basic condition. While the reaction under acidic condition, both of C=C and nitro group of 3- nitrostyrene were hydrogenated to form 3-ethyl nitrobenzene. The 3-vinylaniline about 90% yield was obtained from Pt supported on CNTs with ionic liquid (basic condition) compared to the reaction without ionic liquid which provided 3-vinylaniline about 40% yield.

Pisduangdaw, S., *et al.* (2015) [24] investigated the flame-made Pt/TIO_2 catalysts for the liquid phase selective hydrogenation of 3-nitrostyrene. The effects of reduction temperature from 200 ℃ to 700 ℃ on catalytic performance were also studied. The activity and 3- vinylaniline (3-VA) selectivity increased from 61-66 % and from 40-73% respectively by reduction catalyst at higher temperature (200 ℃ to 600 ℃). According to CO-chemisorption and CO-IR results, reduction catalyst at 500 ℃ and 600 ℃ increased the amount of Pt active sites and decreased Pt terrace sites which promoted the 3-VA selectivity. However, when reduction catalyst at 700 ℃ the catalytic activity was decreased due to the excessive decoration of TiO_x species. Compared to the catalyst prepared by impregnation method, the flame-made catalyst contained the amount of rutile phase less than the impregnated - catalyst leading to higher Pt dispersion and catalytic activity.

Yarulin, A., *et al*. (2015) [6] studied the liquid phase hydrogenation of 3-nitrostyrene using Pt nanoparticles supported on ZnO. Pt were deposited on ZnO by ion-exchange method and the catalyst were reduced under H_2 at temperature range 473 K – 773 K before using in the reaction. From H_2 – TPR results, the peak between 450 K – 550 K was related to the the reduction of ZnO which was in contact with Pt. The catalytic results showed 97% of 3-vinylaniline selectivity at about 100% conversion when using the catalyst reduced at 573 K. The intermetallic Pt/Zn active phase formed via reactive metal (Pt)–support (ZnO) interaction enhanced the catalytic performances.

The metal-support interaction provided the electronic interaction between metal and support and modify the surface morphology. The electron shifted from Zn to Pt inhibited the C=C adsorption according to XPS results and partial blocking of unselective Pt by Zn atom according to CO-chemisorption results. Moreover, the comparison of catalytic performance between Pt supported on reducible metal oxides group (TiO_2 and ZnO) and Pt supported on non-reducible metal oxides group (MgO, Al_2O_3) were studied. The non-reducible metal oxides promoted the 3-ethylaniline (3-EA) selectivity (3- VA about 0% at 100% 3-NS conversion) in contrast to the reducible metal oxides group enhanced the 3-vinylaniline (3-VA) selectivity more than 50% at full conversion.

Table 2.1 Summary of the selective hydrogenation of 3-nitrostyrene with various catalysts and conditions.

Researchers	Catalyst	Preparation method	Reaction conditions	Catalytic results
Boronat, M., et al. (2007)	Au/TiO_2 , Au/SiO_2 , Au/C, Au/Fe_2O_3 , Pt/TiO_2 , Pd/TiO_2	Impregnation	0.9 MPa and 120 ℃	Au/TiO_2 had the highest VA selectivity %Selectivity = 96% %Conv = 98.5%
Shimizu, K., et al. (2009)	Au/ γ-Al_2O_3 , Au/SiO_2 , Au/montmorillonite , Au/MgO , Au/C	colloid deposition	8 MPa and 40 ℃	Au supported on γ-Al_2O_3 provided the higher yield than other supports and small Au NPs (2.5 nm) provided the highest activity

				%Conv = 100% and %VA selectivity = 89%
Serna, P., et al. (2009)	Pt/TiO_2 , Au/TiO_2 , $Pt\text{-}Au/TiO_2$	Monometallic by deposition-precipitation and bimetallic by impregnated second metal on monometallic	0.8 MPa at 85 °C and 120°C 0.2 MPa at 40 °C	$Pt\text{-}Au/TiO_2$ had the highest yield at shorter time compared to the monometallic. %Conv=98.5% % VA selectivity = 95.9%
Yoshida, H., et al. (2011)	Pt/TiO_2	Impregnation	4 MPa of H_2 pressure and various CO_2 pressure at 50 °C	%VA selectivity in ethanol is around 60% and did not change with the CO_2 pressure but %VA selectivity in toluene dropped from 40 % to 15% when increased CO_2 pressure from 0.1-10 MPa
Fujita, S.-i., et al. (2011)	Pt/TiO_2	impregnation	4 MPa H_2 pressure and various CO_2 pressure at 50 °C	0.5% wt. Pt/TiO_2 provided %Conv = 64% and %VA-selectivity = 75% while 2% wt. Pt/TiO_2 provided %Conv = 97% and

				%VA-selectivity = 34%
J.Beier, M., et al. (2012)	Pt on various supports (SiO_2 , AL_2O_3, TiO_2 , and CNTs)	Ionic liquid	1 MPa and room temperature	Pt/CNTs provided the highest yield of 3-vinylaniline about 90% with the presence of ionic liquid (basic conditions).
Pisduangdaw, S., et al .(2014)	Pt/TiO_2	Flame spray pyrolysis	4 MPa and 50 °C	%Conv=99.4% %VA selectivity= 53.1% at 30 min
Yarulin, A., et al. (2015)	Pt-Zn/HPS	impregnation	1 MPa and 75 °C	%selectivity = 97% at full conversion
Yarulin, A., et al. (2015)	Pt/ZnO	Ion - exchange	1 MPa and 75 °C	%selectivity = 97% at full conversion

2.3 Solvothermal synthesis

Solvothermal method is a route for synthesis the nanomaterials with different morphologies. The reactions were carried out in sealed containers and the temperatures can be increased to above the boiling point by increasing the autogeneous pressures resulting from heating[25]. The solvothermal method can improve the reactivity and solubility of reactants due to high temperatures and pressures. This method allowed for the precise control over the size, shape distribution and crystallite size of nanoparticles. The morphologies are controlled by changing parameters such as concentrations of precursors, precursors type, solvent type reaction time and reaction temperature [26].

Nam, W. S., *et al.* (2003) [27] reported the synthesis of TiO_2 by solvothermal reaction of tetra-isopropoxide (TTIP) in different alcohol solvents. The factors such as

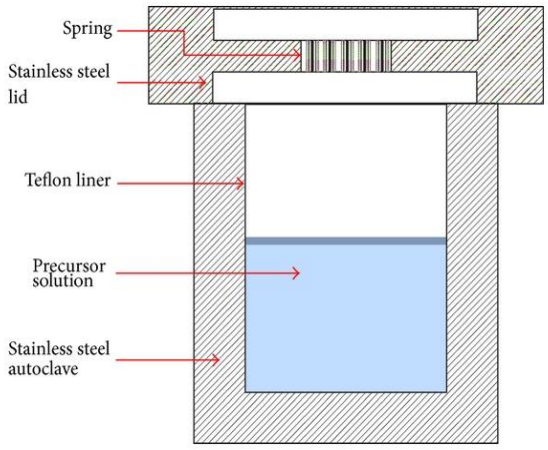

Figure 2.2 Schematic diagram of the autoclave used in solvothermal synthesis [28]

type of solvent and reaction temperature which influenced on the physical properties of TiO_2 were studied. The synthesis TiO_2 powder showed the submicron size and high surface area with a narrow size distribution compared to Degussa P-25 TiO_2 powder. The higher reaction temperature provided the smaller particle size and higher crystallinities

Kim, C.-S., *et al.* (2003) [29] investigated the synthesis of nanocrystalline TiO_2 in toluene with surfactant by solvothermal method. Titanium isopropoxide(TIP) and Oleic acid were used as precursor and surfactant respectively. The effect of molar ratio of TIP: Oleic acid and the weight ratio TIP: toluene to the physical properties of TiO_2 were studied. The anatase nanocrystalline TiO_2 with average crystallite size of 6 nm were obtained after the surfactant-added solution were thermally treated at 250 °C for 20 h in an autoclave. Size distribution of particles synthesized was narrower than particles synthesized without surfactant. Moreover, the sufficient amount of TIP or surfactant can provide the long dumbbell shaped nanorods.

2.4 Study of Pt as catalysts in liquid-phase selective hydrogenation

Platinum (Pt) is an element in group VIII of the periodic table or noble metal. The most common oxidation states are +2 and +4. Pure platinum is a lustrous, ductile,

and malleable, silver-white metal. The other physical properties of Pt are shown in Table1. Platinum is stable at high temperatures and has a great corrosion resistance. It is insoluble in hydrochloric and nitric acid, but dissolves in hot aqua regia to form chloroplatinic acid (H_2PtCl_6Pt has been used in many industries for various applications such as fine jewelry, catalytic converters, electronic devices and catalyst for chemical productions [30]. Pt is always be used in the oxidation and hydrogenation reactions. Pt gives a high activity for H_2 dissociation under mild conditions compared to gold catalysts. However, they were not chemoselective.

Bailón-García.,*et al*. (2016) [8] studied the selective hydrogenation of citral by using noble metal such as Pt, Ru and Ir supported on carbon xerogel. The same metal particle size was obtained after He-pretreatment for comparison between metals. The Pt showed the highest catalytic activity compared to the other metals. Moreover, Pt and Ir exhibited the high selectivity to unsaturated alcohols around 80% more than Ru. Therefore, Pt catalyst is the most appropriate active phase in terms of yield. However, the severe deactivation of Pt catalyst was observed after several runs.

Table 2.2 Physical Properties of Pt [31]

Physical Properties	
Atomic number	78
Atomic weight	195
Electron configuration	$[Xe]4f^{14}5d^{9}6s^{1}$
Electronegativity	2.28
Crystal structure	Face centered cubic (fcc)
Melting point	1768 ℃
Boiling point	3825 ℃

2.5 Effect of Zn-modified catalyst on catalyst properties and catalytic performances

Table 2.3 Physical Properties of Zn [32]

Physical Properties	
Atomic number	30
Atomic weight	65
Electron configuration	$[Ar]3d^{10}4s^2$
Electronegativity	1.65
Crystal structure	Hexagonal close-packed (hcp)
Melting point	419 °C
Boiling point	907 °C

Zn is a blush-white and lustrous transition metal and is the first element of group 12 of the periodic table. The common oxidation states of Zn is 2+.It always loses the two 4s electrons to give a 2+ ion when it forms ions. The other physical properties of Zn are shown in Table 2. They have been used in many applications such as using as an anti-corrosion agent and using as an anode material in batteries. Moreover, Zn have been used to be a promoter or the second metal in the catalyst in hydrogenation reactions[32].

Yarulin, A.,*et al*. (2015) [4] studied the effect of Zn promoted on Pt-based catalysts in liquid phase 3-nitrostyrene hydrogenation to 3-vinylaniline. Pt-Zn catalyst are supported on hypercross-linked polystyrene (HPS).The catalyst results showed that the Zn-modified catalyst provided high 3-vinylaniline selectivity(97%) compared to the unmodified one(16%).Zn modification promoted a stronger shift of electron density

towards Pt which caused the lower adsorption energy of (C=C) bond inhibited the hydrogenation of (C=C) to (C-C). However, the catalytic activity of Pt-Zn catalyst were lowered than the unmodified catalyst because the lower concentration of Pt active sites on the surface which were diluted by non-active Zn.

Bidaoui,M.,*et al*. (2015) [33] studied the improvement of α,β unsaturated aldehyde selective hydrogenation to unsaturated alcohol by using Pt/SBA-15 and Zn-modified Pt/SBA-15.The Zn-modified catalyst were prepared by co-impregnation method at different Zn/Pt atomic ratios. The liquid phase catalytic performance were reported and found that Zn addition increased the selectivity to unsaturated alcohols until maximum at 75% obtained for 0.3 wt.% Zn compared with the unmodified one around 5%. Zn modified improved the adsorption between C=O and C=C bonds. However, the Zn addition led to a lower activity by poisoning the Pt atoms, decreasing the active surfaces.

2.6 Effect of La-modified catalyst on catalyst properties

Table 2.4 Physical Properties of La [34]

Physical Properties	
Atomic number	57
Atomic weight	139
Electron configuration	$[Xe]5d^16s^2$
Electronegativity	1.10
Crystal structure	Double hexagonal close-packed (dhcp)
Melting point	920 °C
Boiling point	3464 °C

Lanthanum (La) is a soft ductile, silvery-white metallic chemical element. It is one of the most reactive of the rare-earth metals: it oxidizes rapidly in air and it reacts with water to form hydroxide. Moreover, La is easily ignited and its salts are often very insoluble. It is considered the first element of the 6^{th} period transition metals. The common oxidation state is 3+. La is usually used in many applications such as catalysts, additives in glass, carbon lighting for studio lighting and projection in lighters and torches[34].

Chen, X.-M., *et al.* (2014) [35] studied the La-modified mesoporous TiO_2 nanoparticles with enhanced photocatalytic activity for elimination of VOCs. The La-modified mesoporous TiO_2 were synthesized via sol-gel method. The XRD patterns results exhibited that the increasing of La content inhibited the transformation of TiO_2 anatase phase to TiO_2 rutile phase with smaller crystallite size. From N_2-physisorption results, the higher La content gives the higher surface area at the same calcined temperature due to the smaller TiO_2 crystallite size. The synthesized catalysts showed the photocatalytic activity compared to commercial catalysts (Degussa, P25).

2.7 Study effect of reduction temperature on catalyst properties and catalytic performance

Corma, A., *et al*. (2008) [9] reported the method for transforming nonchemoselective metal catalyst to selective ones by controlling the coordination of metal surface atom. Pt/TiO_2 was reduced at 473 K and 773 K. Under 473 K, the fraction of highly coordinates Pt (Pt terrace sites) were found much more than low coordinates Pt sites like steps and corners which provides low selectivity to vinylaniline. In contrast, the low coordinates Pt sites are presence without Pt terrace sites causes high selectivity to vinylaniline at 773 K.

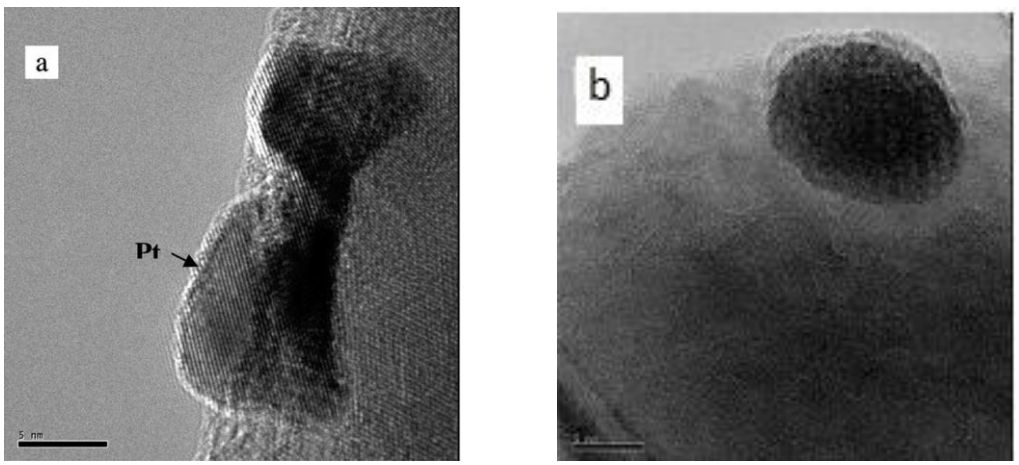

Figure 2.3 a) HRTEM images of 0.2 wt% Pt/TiO_2 catalyst after reduction at 473 K. The surface of the crystallites appears free from any support material b) HRTEM images of 0.2 wt % Pt/TiO_2 catalyst after reduction at 723 K. The Pt particle surface appears partially covered by TiO_x species as a decoration effect.[9]

S. A. Ananthan., *et al.* (2013) [36] studied the selective hydrogenation of citral to unsaturated alcohols using TiO_2 supported Pt based bimetallic. The bimetallic catalysts, Pt-Ru, Pt-Au and Pt-Pd were prepared by impregnation and reduced under H_2 at two different temperatures, 375 ℃ and 575 ℃. The catalysts which reduced at higher temperature provided a SMSI effect due to TiO(2-x) species. The SMSI effects led to an increasing of unsaturated alcohols selectivity during the citral hydrogenation.

2.8 Study the CO adsorption on Pt catalyst

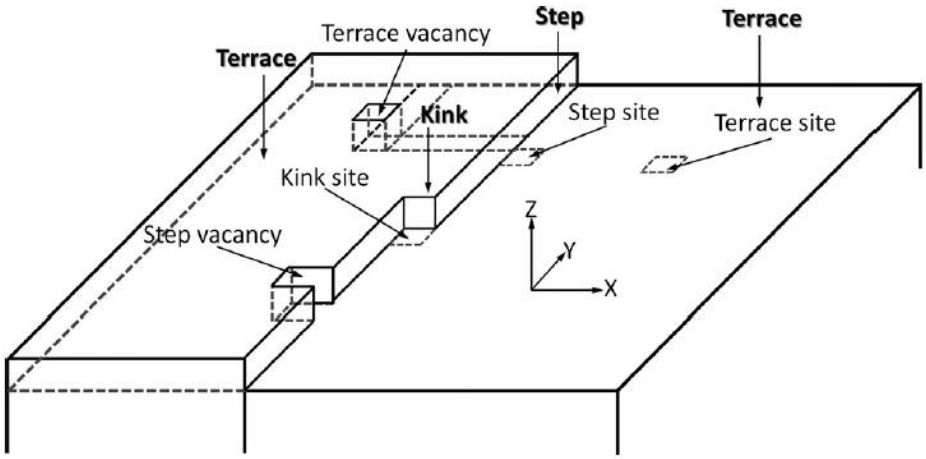

Figure 2.4 Schematic diagram of the substrate surface described by the Kossel–Stranski "terrace–step–kink" model. [37]

In the 19th century several hydrocarbon reactions over platinum catalysts were studied as a function of the catalyst particle size. The reactions like alkane hydrogenolysis and isomerization were strongly dependent on the particle size called structure sensitive while reactions like cyclopropane ring opening and olefin hydrogenation were independent of the particle size called structure insensitive.[38] The crystal structure of metal atom are shown in Figure 2.4. The relative concentration of terrace, step and kink was changed with the metal particle size.

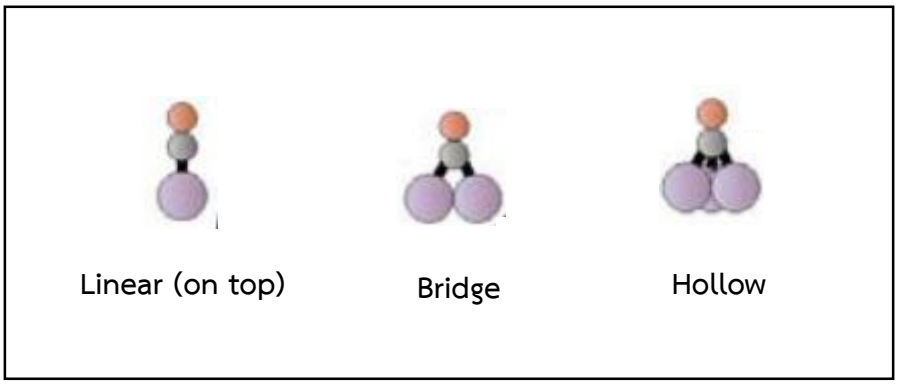

Figure 2.5 Types of CO adsorption on metal surfaces

Fourier transform infrared (FTIR) spectroscopy of the CO adsorption is always utilized for surface of catalyst characterization. The CO stretching frequency is sensitive to the structure surface and decreases relative to the gas phase frequency due to changes in surface atom coordination.[39] There are three types of CO adsorption behaviors on Pt clusters as 1) linear CO adsorption 2) bridge CO adsorption 3) hollow CO adsorption or multi-bonded CO adsorption. The linear CO adsorbed predominates on small metal particles while the bridged CO adsorbed on larger metal particles. [40] Corma, A., *et al* (2008) [9] reported the method for transforming non-chemoselective metal catalyst to selective ones by controlling the coordination of metal surface atom. For 3-nitrostyrene hydrogenation, the smaller fraction of Pt terrace sites to corner sites tend to decreased the rate of structure sensitive reaction as C=C double bond while maintaining the activity for the reduction of nitro group. The high fraction of Pt corner sites to Pt terrace sites was observed when the catalyst reduced at high temperature (773 K) favored the 3-vinylaniline selectivity.

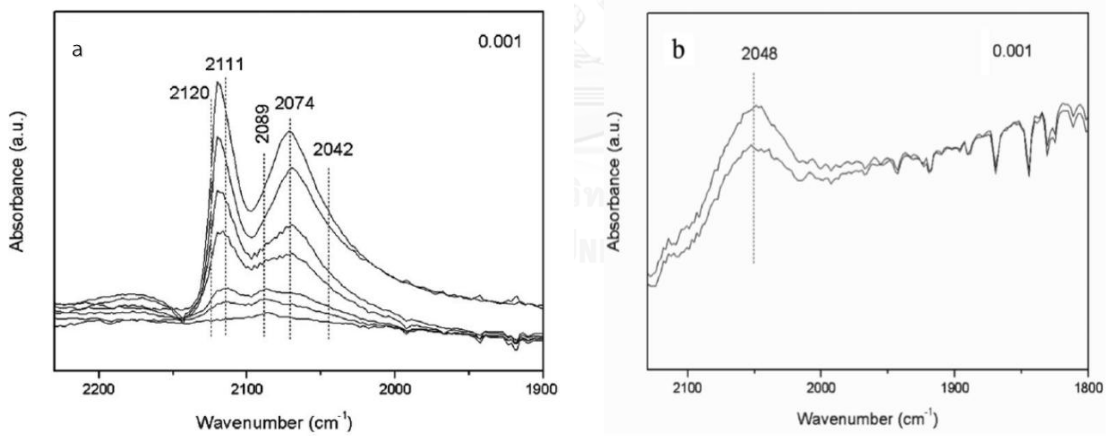

Figure 2.6 a) IR spectra of CO adsorbed on this sample which reduced at 473 K reveal the presence of Pt terraces Pt(111) and Pt(100), as well as oxidized metal sites b) IR spectra of CO adsorbed on this sample which reduced at 723 K showed only one band corresponding to low surface coordination sites, indicating the absence of Pt terraces Pt(111) and Pt(100). [9]

Figure 2.6 a) shows the CO-IR spectra of 0.2 wt.% Pt/TiO_2 which reduced at 473 K. The high-frequency band at 2120 cm^{-1} has been assigned to CO adsorbed on oxidized Pt surface sites, while IR bands in the 2111-2086 cm^{-1} region correspond to CO molecules adsorbed on Pt(111) terraces (sites with coordination number 9). The IR bands in the 2077-2071 cm^{-1} region have been related to CO molecules adsorbed on Pt(100) (Pt sites with coordination number 8). The IR bands at lower frequencies (2066, 2050, and 2040-2020 cm^{-1}) indicate the presence of Pt sites of low surface coordination, like steps and corners. While the same catalyst which reduced at 723 K, only one band at 2048 cm^{-1} due to CO adsorption on Pt-Ti interface sites and none of Pt terrace sites adsorption band was observed. The high fraction of Pt corner sites to Pt terrace sites favored the 3-vinylaniline selectivity.

CHAPTER III
EXPERIMENTAL

This chapter explains about the materials and procedures in this research including the catalyst preparation, catalyst characterization by various techniques and measurement of catalytic performances in the liquid phase selective 3-nitrostyrene hydrogenation.

3.1 Materials

Table 3.1 List of chemicals used for catalyst preparation and catalytic performance

Chemical substances	Suppliers
Titanium n-butoxide	Arcos
1,4-butanediol	Sigma Aldrich
Zinc acetylacetonate	Merck
Lanthanum (III) nitrate hexahydrate	Sigma Aldrich
Methanol	Sigma Aldrich
Chloroplatinic acid	Sigma Aldrich
3-nitrostyrene	Sigma Aldrich
Vinylaniline	Sigma Aldrich
Ethylaniline	Sigma Aldrich
Ethanol	Merck
Decane	Sigma Aldrich

3.2 Catalyst Preparation

3.2.1 Synthesis of TiO_2 support and Zn and La-modified TiO_2 supports

TiO_2 were prepared and modified by the solvothermal method according to the method described in Ref[41]. Titanium n-butoxide (TNB) and 1,4-butanediol were used as TiO_2 precursor and organic solvent, respectively. Firstly, 25 g of TNB was dissolved in 100 cm^3 of 1,4-butanediol. Then mixed solution in the test tube and 30

cm^3 1,4-butanediol was filled into the outer tube and putted them into the 300 cm^3 autoclave. The nitrogen gas was purged into the autoclave reactor before heating up to 320 ºC at a rate of 2.5 ºC/min and held constant at that temperature for 4 h. The Zn-doped TiO_2 and La-doped TiO_2 were prepared by addition the desired amount of zinc acetylacetonate or Lanthanum (III) nitrate hexahydrate into the mixed solution before setting up in the autoclave. The molar ratios of Zn/Ti and La/Ti were 0.005, 0.01, and 0.02. After cooling to room temperature, the products were washed with methanol and dried in air.

3.2.2 Synthesis of Pt/TiO_2, Pt/Zn-modified TiO_2 and Pt/La-modified TiO_2 catalysts

The Pt/TiO_2 and Pt/Zn and La-modified TiO_2 catalysts were prepared by incipient wetness impregnation. Chloroplatinic acid hydrate were dissolved into DI water and dropped into TiO_2, Zn and La-modified TiO_2 equal to pore volume of support to obtain 0.5% wt Pt loading. Then the catalysts were dried in room temperature for 6 h and dried in oven at 110°C overnight. The dried catalysts were subsequently calcined in air at 450 °C for 4 h. Finally, the catalysts were reduced at 200 °C or 500 °C under H_2 flow 50 cm^3/min for 3 h.

3.2.3 Synthesis of sequential-impregnation Pt/Zn and La-modified TiO_2 and co-impregnation Pt/Zn and La-modified TiO_2

For sequential-impregnation catalysts, zinc acetylacetonate solution or Lanthanum (III) nitrate hexahydrate were dropped into TiO_2 to obtain the optimum ratio of Zn/Ti or La/Ti and then Pt solution were dropped consequently into modified TiO_2 to obtain 0.5% wt Pt loading. Then the catalysts were dried in room temperature for 6 h and dried in oven at 110°C overnight. The dried catalysts were subsequently calcined in air at 450 °C for 4 h.

For co-impregnation catalysts, the mixture of zinc acetylacetonate with Chloroplatinic acid hydrate at the optimum ratio of Zn/Ti were dropped into TiO_2 to obtain Pt/Zn-modified TiO_2 and the mixture of Lanthanum (III) nitrate hexahydrate with Chloroplatinic acid hydrate at the optimum ratio of La/Ti were dropped into TiO_2 to

obtain Pt/La-modified TiO_2. Then the catalysts were dried in room temperature for 6 h and dried in oven at 110°C overnight. The dried catalysts were subsequently calcined in air at 450 °C for 4 h.

3.3 Measurement of catalytic performance in liquid phase selective 3-nitrostyrene hydrogenation

The liquid phase selective 3-nitrostyrene hydrogenation were performed isothermally at 40 °C under H_2 pressure 20 bar for 60 min in 50 cm^3 autoclave reactor. The reactor was charged with the catalyst 20 mg and mixture of 3-nitrostyrene 0.5 cm^3 with ethanol 10 cm^3. Then the reactor was purged with H_2 gas for 4 times to eliminate air. The timer was started when the mixture was stirred with magnetic stirrer. The reactor was depressurized after the reaction and cooled down by ice water to stop the reaction. Finally, the products were analyzed by a gas chromatograph attached with a flame ionization detector.

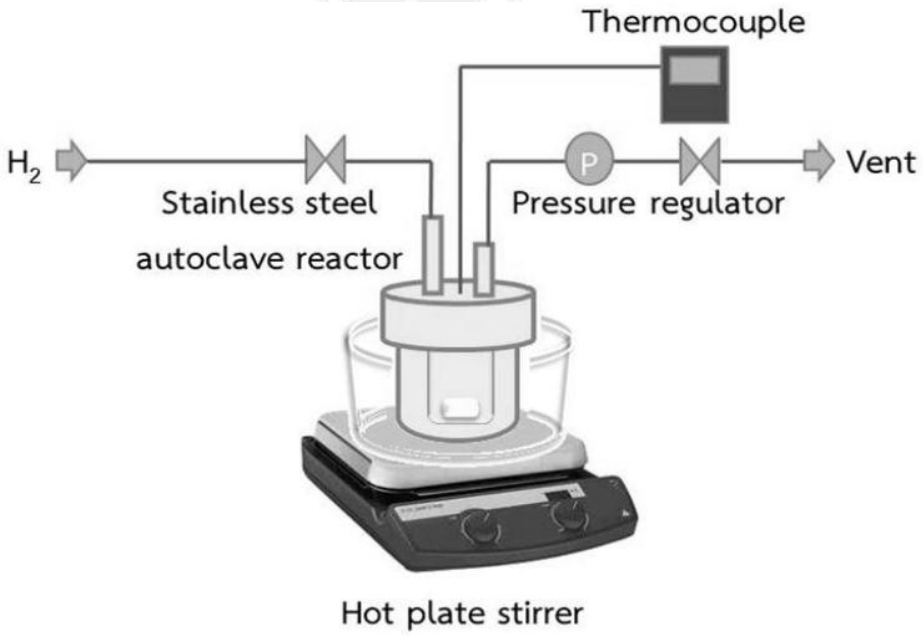

Figure 3.1 The schematic diagram of liquid-phase hydrogenation[42].

Table 3.2 Gas-Chromatography operating conditions

Gas chromatography(Shimadzu GC-2014)	Conditions
Detector	FID
Packed column	Rtx®5
Carrier gas	Helium (99.99 vol.%)
Make-up gas	Air (99.9 vol.%)
Column temperature	140 °C
Injector temperature	270 °C
Detector temperature	310 °C
Time analysis	30 min

3.4 Catalyst Characterization

X-ray diffraction (XRD)

The XRD patterns and crystallite size of all the supports and catalysts were detected by the SIEMENS D5000 x-ray diffractometer using Cu K_α radiation with Ni filter in the 2θ range of 20° to 80° and resolution 0.04°. The crystallite size of catalysts were calculated by Scherrer equation and using α-alumina as the external standard.

N_2-physisorption

N_2-physisorption are used for determining surface area (BET method), average pore size diameter and average pore volume (BJH model). All of the support and catalysts were analyzed by using the Micromeritics Pulse Chemisorb 2750 instrument. The samples were thermally treated for 3 h at 180 $^\circ$C before analysis. The nitrogen adsorption-desorption isotherms at -196 $^\circ$C under liquid nitrogen.

CO-Pulse Chemisorption

CO-pulse chemisorptions are utilized for determining the amount of Pt active sites and the percentages dispersion of Pt/TiO_2 and $Pt/Zn\text{-}TiO_2$ catalysts using MicromeriticsChemisorb 2750. Prior to pulsing CO over the catalyst, approximately 0.05 g of catalyst was reduced under H_2 flow rate 50 ml/min at 200°C or 500°C for 3h. The CO was pulsed over the catalyst at 30°C until the TCD signals are constant. The constant TCD signals correspond to none of CO are further adsorp on Pt active sites. The percentages dispersion are calculated by assuming that one molecule of CO adsorps on one molecule of Pt and none of CO molecule adsorps on Zn sites.

H_2-temperature program reduction (H_2-TPR)

The catalyst reduction behaviors are determined by H_2-TPR measurements which performed in a quartz U-tube reactor. The catalyst pretreatment are carried out in a N_2 flow rate 25 ml/min at 450°C for 1h. The catalyst are reduced under 10%H_2 in He flow rate 25 ml/min ramping from 30 to 800 °C at heat rate 10°C/min using a Micromeritics AutochemiSorb 2910 system attached with ChemiSoft TPx software.

X-ray photoelectron spectroscopy (XPS)

The XPS spectra, the blinding energy, full width at half maximum (FWHM) and the composition of the Pt catalysts on the surface layer of the catalysts were performed by using the Kratos Amicus x-ray photoelectron spectroscopy. The experiment was operated with the x-ray source at 20 mA and 12 kV (240 W), the resolution at 0.1 eV/step and the pass energy of the analyzer was set at 75 eV under pressure approximately 1x10-6 Pa. For calibration, the blinding energy was referenced to C 1s line at 285.0 eV. The blinding energy of O 1s, Ti 2p and Pt 4f are determined.

Transmission electron microscopy (TEM)

The transmission electron microscope of JEOL JEM-2010 equipped with LaB_6 thermolonic electron gun operating at voltage 120 kV was employed for TEM analysis. This technique provided TiO_2 crystallite size and morphology images.

FT-IR analysis for CO adsorbed on the catalyst (CO-IR)

This technique was used to analyze the coordination of Pt surface by CO adsorption on the Pt surface. The FTIR spectrometer (Bruker) with a liquid nitrogen-cooled MCT detector was used in this analysis. The catalysts were pressed into the pellets and placed in a temperature-controlled flow cell. Prior to reduce the catalysts, the remaining air in sample cell was purged with He gas. The sample was reduced at two different temperatures (200 °C and 500 °C) in H_2 flow for 1 hr before cooling to 30 °C. The background spectrum was then taken in He flow before the CO adsorption to substracted the effects of TiO_2. The CO gas was introduced into the sample cell for 15 min and then was purged with He to eliminate the CO gas phase and physisorbed CO. The FTIR spectra were recorded in the 400-4000 cm^{-1} range at a wavenumber resolution of 4 cm^{-1} and 150 scans.

CHAPTER IV
RESULTS AND DISCUSSION

This chapter describes about the characteristics and catalytic properties of Pt catalysts supported on Zn and La-modified TiO_2 in the selective hydrogenation of 3-nitrostyrene. The effects of reduction temperature and the effect of amount of promoter on Pt catalysts were investigated. Moreover, the effect of catalysts preparation method of the optimum amount of selected promoter were also investigated. The catalysts were characterized by various techniques such as XRD, N_2-physisorption, XPS, TEM, H_2-TPR, CO-chemisorption and CO-IR.

4.1 The effects of amount of Zn on the properties of TiO_2 and Pt catalysts supported on Zn-modified TiO_2 supports.

4.1.1 Catalysts Characterization

4.1.1.1 X-ray diffraction (XRD)

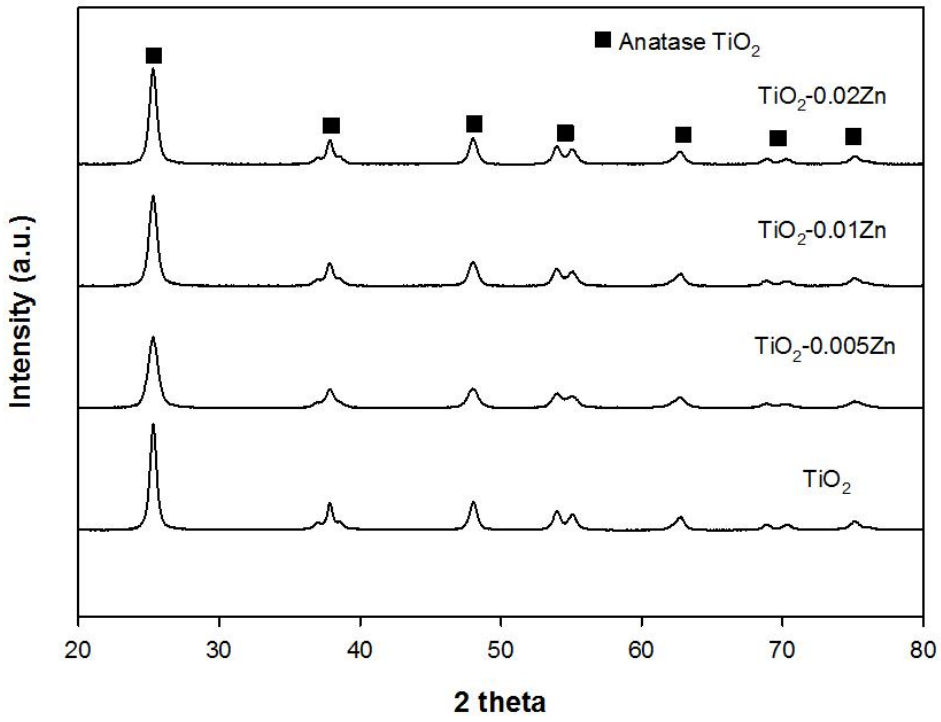

Figure 4.1 XRD patterns of TiO_2 and Zn-modified TiO_2

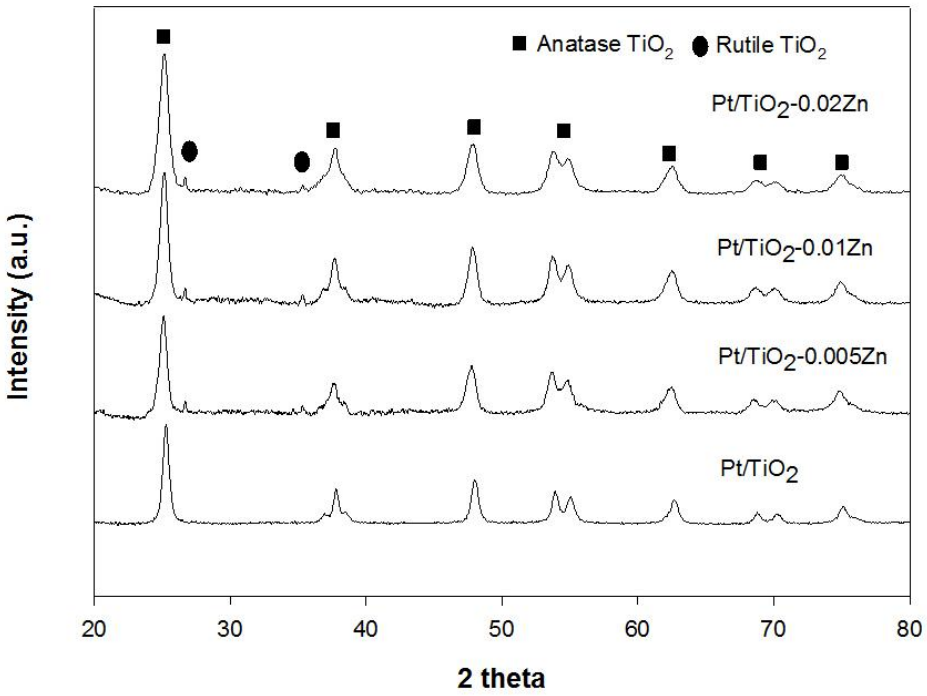

Figure 4.2 XRD patterns of Pt/TiO_2 and Pt/Zn-modified TiO_2 catalysts

The TiO_2 and Zn-modified TiO_2 were prepared by solvothermal method and Pt catalysts were prepared by incipient wetness impregnation method. The XRD patterns of TiO_2 and Zn-modified TiO_2 are shown in Figure 4.1. The characteristic peaks of anatase phase TiO_2 were observed at 2θ 25°(anatase major peak), 37°, 49°, 54°, 63°, 69° and 75° in all supports.

The XRD patterns of the Pt/TiO_2 and Pt/Zn-modified TiO_2 are shown in Figure 4.2. The anatase phase TiO_2 were observed in all the catalysts. Rutile phase TiO_2 were additionally observed at 28°(major rutile peak) and 36° in the Pt/Zn modified TiO_2.The characteristic peaks of Pt species were not detected due to low Pt loading and/or good dispersion of Pt on TiO_2 support.

4.1.1.2 N_2-physisorption

From N_2 adsorption-desorption isotherms, the average pore sizes of all the catalysts were in range of 11-14 nm corresponding to the mesoporous structure (2-50 nm) as shown in Figure 4.3

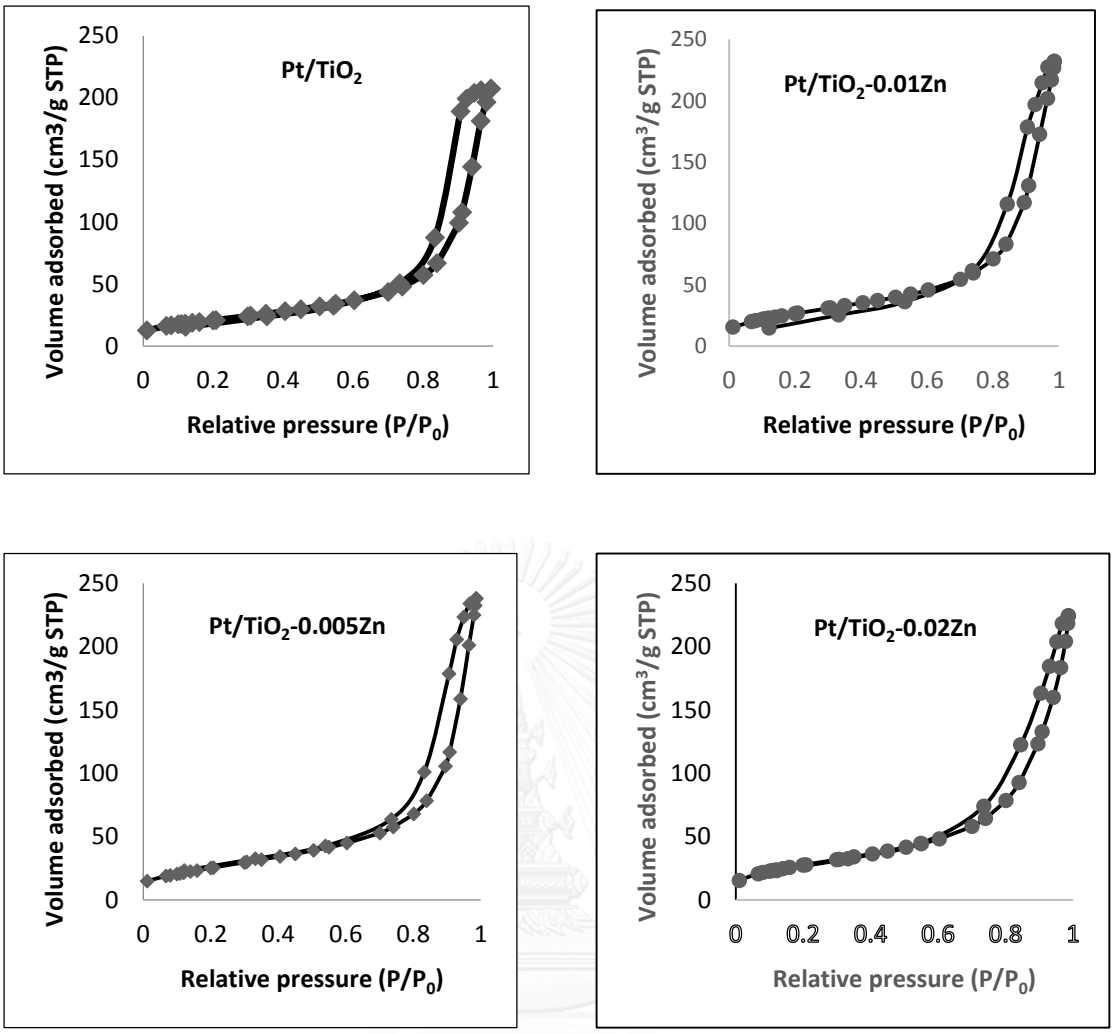

Figure 4.3 N_2 adsorption-desorption isotherms at -196 ℃ of Pt/TiO_2 and Pt/TiO_2-modified Zn at various amount of Zn

Table 4.1 Physical properties of TiO_2 and Zn-modified TiO_2.

Support	BET surface area (m^2/g)	Average pore diameter (nm)	Pore volume ($cm^3(STP)/g$)	TiO_2 Crystallite size (nm)
TiO_2	83	14.5	0.38	16.5
TiO_2-0.005Zn	75	11.5	0.32	13.8
TiO_2-0.01Zn	85	12.8	0.33	12.5
TiO_2-0.02Zn	85	14.3	0.36	10.5

The physical properties of TiO_2 and Zn-modified TiO_2 are shown in Table 4.1. The surface area of unmodified TiO_2 and Zn-modified TiO_2 were around 80 m^2/g. The TiO_2 crystallite size of unmodified TiO_2 and Zn-modified TiO_2 were calculated by Scherrer equation. The TiO_2 crystallite size were decreased with the increasing of amount of Zn from 16.5 nm to 10.5 nm. According to Aware D.V. [43] et al., preparing Zn-doped TiO_2 by sol-gel method .When the mol% of the zinc ion doping in TiO_2 was increased, the crystallite size decreased.

Table 4.2 Physical properties of Pt/TiO_2 and Pt/Zn-modified TiO_2 catalysts.

Catalyst	BET surface area (m^2/g)	Average pore diameter (nm)	Pore volume ($cm^3(STP)/g$)	TiO_2 Crystallite size (nm)
Pt/TiO_2	75	13.5	0.32	16.0
Pt/TiO_2-0.005Zn	93	11.3	0.37	12.1
Pt/TiO_2-0.01Zn	98	11.0	0.35	11.2
Pt/TiO_2-0.02Zn	101	10.1	0.35	10.4

The BET surface area, average pore size, pore volume and hyteresis of Pt catalysts supported on TiO_2 and Zn-modified TiO_2 were determined by N_2-physisorption.The physical properties of Pt catalysts are shown in Table 4.2. The BET surface area of Pt/TiO_2 was around 75 m^2/g. The BET surface area of Zn-modified catalysts were higher than the unmodified one and were increased from 93 m^2/g to 101 m^2/g with increasing molar ratios of Zn/Ti from 0.005 to 0.02. Although, rutile occured in the modified catalysts, the surface areas were higher than the unmodified one because the crystallite size of anatase phase was smaller than the unmodified catalyst.

4.1.1.3 H_2-temperature programmed reduction

The reduction behaviors of catalysts were determined by H_2-TPR. The H_2-TPR profiles are shown in Figure 4.4. The first peak was related to the reduction of Pt oxide particles. The second peak was attributed to Pt-TiO_x interface sites reduction and the last one above 500 °C was associated to the reduction of surface capping oxygen of TiO_2 [24].

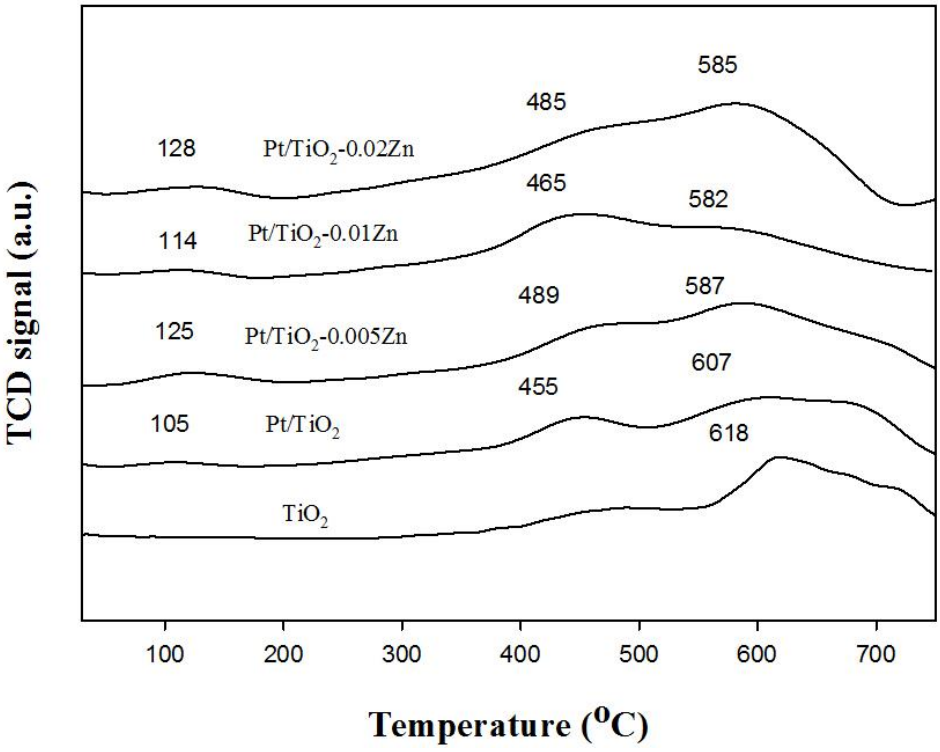

Figure 4.4 H_2-TPR profiles of TiO_2, Pt/TiO_2 and Pt/Zn-modified TiO_2

For the Pt/Zn-modified TiO_2, the first peak was shifted to higher temperature than the unmodified catalyst, suggesting a larger particle of Pt and/or lower reducibility. Furthermore, the second peak of Pt/Zn-modified TiO_2 was also shifted to higher temperature than the unmodified catalyst suggesting a stronger interaction between Pt and TiO_2 or/and between Pt and Zn. Moreover, the third peak of Pt supported on TiO_2 or Zn-modified TiO_2 were lower than the TiO_2 due to spillover of H_2 to TiO_2 surfaces[44].

4.1.1.4 CO-chemisorption

The Pt dispersion or the amount of Pt active sites were evaluated by CO-chemisorption. All the catalysts were reduced under H_2 flow at 200 ℃ before CO injection to adsorb on active sites. The %Pt dispersion were determined by assuming that one molecule of CO adsorbed on one molecule of Pt and none of CO molecule adsorbed on Zn sites. The % Pt dispersion and amount of active sites of Pt/TiO_2 and Pt/Zn-modified TiO_2 are shown in Table 4.3. The amount of active sites were decreased because of the dilution of Pt surfaces by Zn[45].

Table 4.3 %Pt dispersion and amount of active sites of catalysts which reduced at 200 ℃.

Catalysts	%Pt dispersion	Amount of active sites ($x10^{18}$) ($x10^{18}$ molecule CO/g cat)
Pt/TiO_2	69	10.6
Pt/TiO_2-0.005Zn	55	8.4
Pt/TiO_2-0.01Zn	54	8.3
Pt/TiO_2-0.02Zn	37	5.7

4.1.1.5 X-ray photoelectron spectroscopy (XPS)

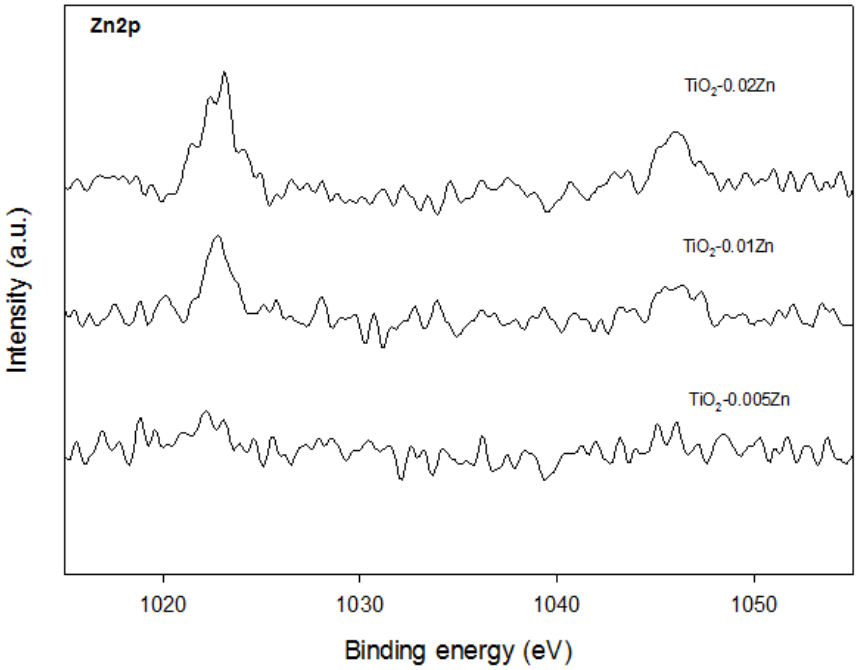

Figure 4.5 XPS spectra of Zn2p of Zn-modified TiO_2

X-ray photoelectron spectroscopy (XPS) is a technique that always use to confirm the presence of element. The XPS spectra of Zn of the Zn-modified TiO_2 are shown in Figure 4.5. The peaks at around 1023 and 1046 eV were related to Zn $2p_{3/2}$ and Zn $2p_{1/2}$. The difference between these two spectra about 23 eV corresponding to Zn^{2+}[46]. The higher intensity of spectra were observed when increased the molar ratio of Zn/Ti.

The Ti spectra of TiO_2 and Zn-modified TiO_2 are shown in Figure 4.6. There are two peaks at around 459 eV and 464.6 eV which corresponded to the $Ti2p_{3/2}$ and $Ti2p_{1/2}$, respectively[47]. These values were corresponding to the Ti^{4+}. Two separation peaks were consistent with the oxide values which energy gap between them about 5.7 eV related to the oxide. The $Ti2p_{3/2}$ of Zn-modified catalyst were shifted to higher binding energy when the amount of zinc were increased. The ion radius of Zn^{2+} (0.074 nm) is larger than the Ti^{4+} (0.068 nm) so it is difficult that Zn entered to the TiO_2 lattice in substitutional or interstitial mode [47-49]. Therefore, Ti atoms may be replaced by the Zn atoms on the interface of TiO_2 crystal in form Ti-O-Zn.

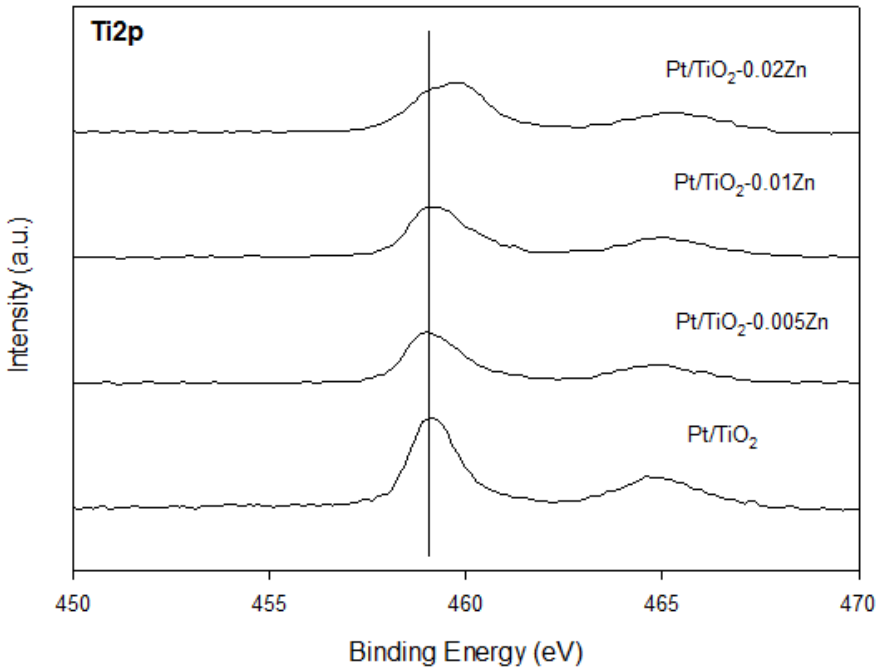

Figure 4.6 XPS spectra of Ti2p of Pt/TiO_2 and Pt/Zn-modified TiO_2

4.1.1.6 Transmission electron microscope (TEM)

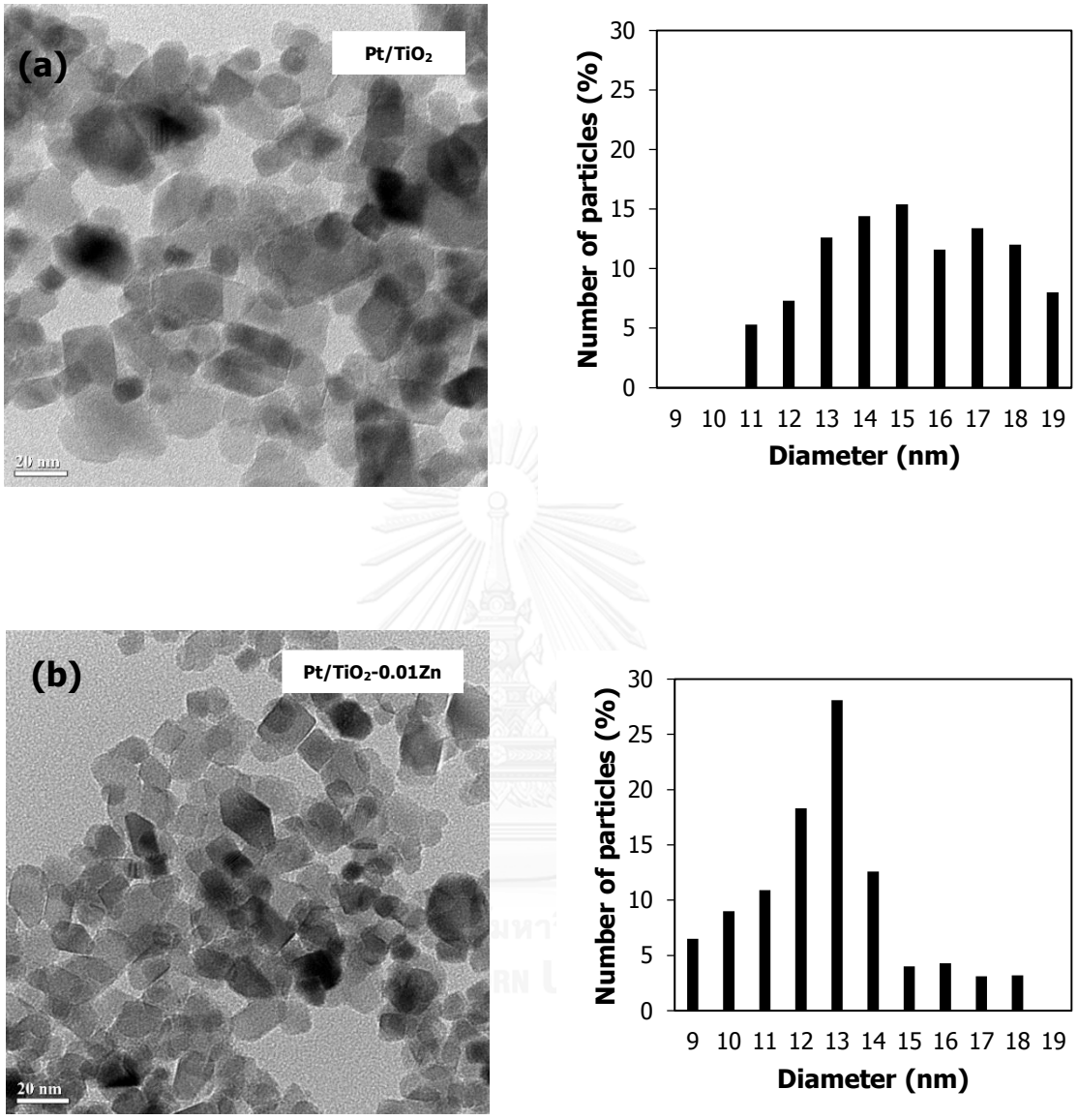

Figure 4.7 TEM images and the size distribution of (a) Pt/TiO_2 and (b) Pt/TiO_2.-0.01Zn

The morphology of catalysts can be attained by transmission electron microscope (TEM). TEM images and size distribution of Pt/TiO_2 and Pt/TiO_2-0.01Zn are show in Figure 4.7. Both of catalysts showed non-spherical shapes. The TiO_2 particle size of Pt/TiO_2 were uniformly distributed in range of 11-19 nm compared to the particle size of the Pt/TiO_2-0.01Zn which major size were in range of 12-14 nm. Pt particles could not be detected due to low metal loading or good dispersion.

4.2.1.2 FT-IR analysis for CO adsorbed on the catalyst (CO-IR)

In order to further study the effects of the presence of Zn on the sites of dispersed Pt particles and for the catalytic performance, CO adsorption on the unmodified catalyst and Zn-modified catalyst was investigated with in-situ FT-IR technique. The coordination of Pt surface atom can be detected by using CO-IR technique. The adsorption bands occurred in different frequency which depended on the sites of Pt. The adsorption band at around 2050 cm^{-1} related to the linear CO adsorption while the absorption band at 2070 – 2100 cm^{-1} may be the absorption of CO adsorbed on highly coordinated Pt surfaces like Pt(111) and Pt(100) and at 2000 – 2066 cm^{-1} on low coordinated Pt sites like kink, edge, and corner[9]. Figure 4.8 illustrates the FTIR spectra of adsorbed CO over the Pt/TiO_2 and Pt/TiO_2-0.01Zn which were reduced at 200 °C. The spectra band at wavenumber 2062 and 2066 cm^{-1} were related to the low coordinated Pt sites and there was no peaks showing the Pt terrace sites. The relative quantity of Pt edge sites over Pt/TiO_2 was higher than the Pt/TiO_2-0.01Zn.

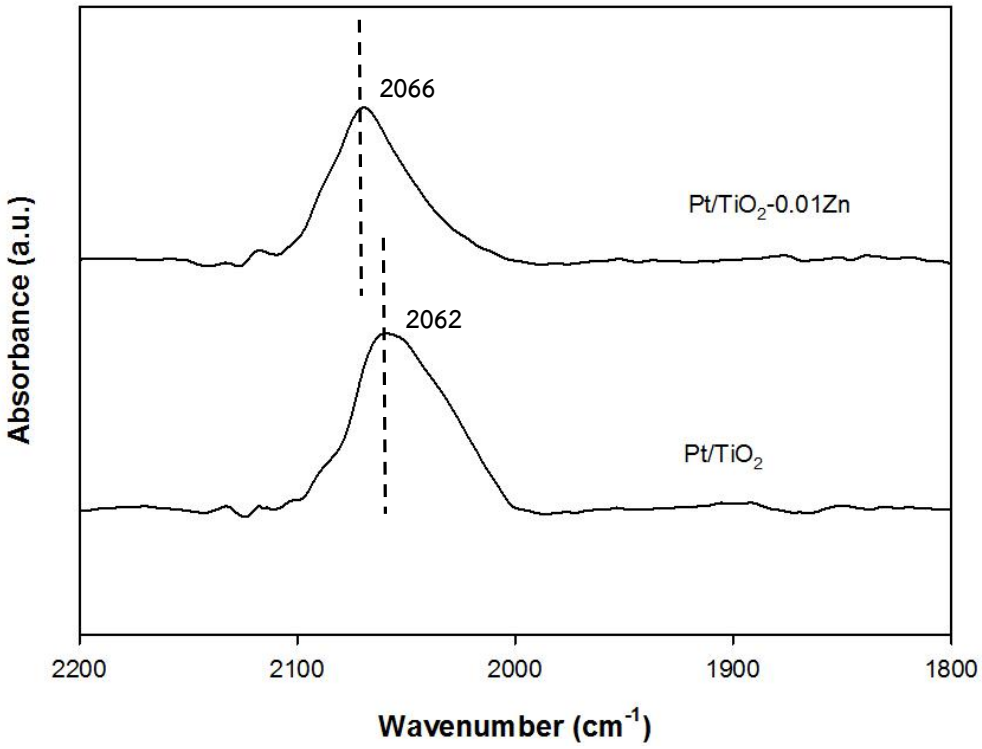

Figure 4.8 FTIR spectra of adsorbed CO over Pt/TiO_2 and Pt/TiO_2-0.01Zn which reduced at 200 °C

4.1.2 Catalytic performances of Pt/Zn-modified TiO_2 in the liquid phase selective hydrogenation of 3-nitrostyrene

The catalytic measurements of Pt catalysts supported on TiO_2 and Zn-modified TiO_2 at various amounts of Zn were evaluated in the liquid phase selective hydrogenation of 3-nitrostyrne. Prior to the reaction, the catalysts were reduced under H_2 flow at 200 °C. The reaction were carried out batchwise isothermally at 40 °C under H_2 pressure 20 bar for 60 min. The products of liquid phase selective hydrogenation of 3-nitrostyrene were analyzed by a gas-chromatograph. The catalytic results such as activity and VA-selectivity are shown in Table 4.4. 3-nitrostyrene conversion is defined as the moles of 3-nitrostyrene converted with respect to the moles of 3-nitrostyrne initial. 3-VA selectivity is defined as the ratio of the amount of 3-VA occurred to amount of all products. The Pt/TiO_2 shows the highest conversion about 80% and the conversion were dropped when the Zn content in catalysts were increased. The Pt surfaces were diluted by the presence of non-active Zn or allowed less Pt surfaces atom (as shown by chemisorption) caused the low conversion of Pt/Zn-modified TiO_2 [45, 50].

The product selectivity of this reaction strongly depended on the Pt surface atom. According to Corma *et al*.[9], rate of C=C hydrogenation was decreased by increasing the ratio of Pt corner/edge sites to Pt terrace sites. Therefore, the VA selectivity of Pt/TiO_2-0.01Zn was lower than the Pt/TiO_2 due to the less quantity of low coordinated Pt sites according to CO-IR results which shown in Figure 4.8.

Table 4.4 Reaction results of the Pt/TiO_2 catalysts Pt/Zn-modified TiO_2 catalysts

Catalyst	Conversion (%)[a]	VA selectivity(%)[a]	Yield (%)	Dispersion(%)[b]
Pt/TiO_2	80	77	61	69
Pt/TiO_2-0.005Zn	79	80	63	55
Pt/TiO_2-0.01Zn	43	65	28	54
Pt/TiO_2-0.02Zn	26	68	18	37

4.2 The effects of reduction temperature on the properties of Pt catalysts supported on Zn-modified TiO_2 supports

4.2.1 Catalyst Characterization

4.2.1.1 CO-chemisorption

CO-chemisorption was used to determined %Pt dispersion or amount of actives sites. Prior to adsorb CO on catalysts, the catalysts were reduced under H_2 flow at 200 °C and 500 °C. At low reduction temperature, %Pt dispersion of all catalysts were higher than the catalysts reduced under high reduction temperature which shown in Table 4.5.

At high reduction temperature, the Zn-modified catalyst exhibited good dispersion than the unmodified catalysts. The dispersion was increased when adding molar ratio of Zn/Ti from 0.005 and 0.01 but the dispersion was decreased when the molar ratio is 0.02.

Table 4.5 CO-chemisorption of Pt/TiO_2 and Pt/Zn-modified TiO_2 catalysts

Catalysts	Reduction temperature (°C)	%Pt dispersion	Amount of active sites (x10^{18} molecule CO/g cat)
Pt/TiO_2	200	69	10.6
	500	43	6.7
Pt/TiO_2-0.005Zn	200	55	8.4
	500	58	9.0
Pt/TiO_2-0.01Zn	200	54	8.3
	500	53	8.2
Pt/TiO_2-0.02Zn	200	37	5.7
	500	51	7.9

4.2.2 Effects of reduction temperature on catalytic performances of Pt/Zn-modified TiO_2 in the liquid phase selective hydrogenation of 3-nitrostyrene

Liquid phase selective hydrogenation of 3-nitrostyrene were performed over Pt/TiO_2 and Pt/Zn-modified TiO_2 after low reduction temperature (200 °C) and high reduction temperature (500 °C). The catalytic results such as %conversion and %VA selectivity are shown in Table 4.6. The Pt/TiO_2 which reduced at 200 °C shows the higher conversion than the Pt/TiO_2 which reduced under 500 °C. The product selectivity of 3-nitrostyrene hydrogenation reaction was strongly depended on the nature of Pt surface sites[51]. The VA selectivity of catalysts reduced at 500 °C was higher than the ones at 200 °C. The reduction temperature has the effects on the coordination of metal surface atom. Vinyl group or C=C group hydrogenation is structure sensitive reaction. Therefore, there was an attempt to decreased the rate of C=C hydrogenation by increasing the ratio of Pt corner/edge sites to Pt terrace sites. According to Pisduangdaw et al.[24], the high reduction temperature led to the decreasing of Pt terrace sites. Therefore, the VA selectivity at high reduction temperature was higher than the low reduction temperature due to the increasing of Pt corner/edge sites.

The Pt/Zn-modified TiO_2 which reduced under 200 °C shows the lower conversion than the unmodified ones. The Pt surfaces were diluted by the presence of non-active Zn caused the low conversion of Pt/Zn-modified TiO_2[4]. In contrast to the reduction at 500 °C, all the Zn-modified catalysts showed higher activity than the unmodified catalyst with the Pt/TiO_2-0.005Zn exhibited the highest NS conversion at 64% after 60 min reaction time. Compared to the Pt/TiO_2, the selectivity was slightly decreased from 86% to 80-84% for the Zn modified catalysts with Zn/Ti molar ratio 0.005-0.01. According to the CO chemisorption results, Pt/Zn-modified catalysts gave a superior dispersion than the unmodified ones corresponding to the higher amount of active sites. Moreover, the Zn-modified catalyst at high reduction temperature (500 °C) caused the Pt-Zn strong interaction or PtZn alloy that the electron from Zn was shifted to Pt. According to Yarulin [6], the ZnO reduction occurs in range of 177 °C to 277°C and expected that the higher degree of intermetallic Pt/Zn increased with the reduction temperature. According to H_2-TPR results, the increasing of Zn caused the

Table 4.6 Reaction results of the Pt/TiO_2 catalysts Pt/Zn-modified TiO_2 catalysts at different reduction temperatures

Catalyst	Reduction temperature (°C)	Conv (%)	VA selectivity(%)	Yield (%)	Dispersion (%)
Pt/TiO_2	200	80	77	61	69
	500	44	86	38	43
Pt/TiO_2-0.005Zn	200	79	80	63	55
	500	64	80	51	58
Pt/TiO_2-0.01Zn	200	43	65	28	54
	500	63	84	53	53
Pt/TiO_2-0.02Zn	200	26	68	18	37
	500	54	75	41	51

peak shifted to higher temperature implied a stronger metal support interaction. At high reduction temperature, the VA selectivity were maintained at relatively high level due to the decoration of Pt surface atoms by TiO_{2-x}, increasing number of low coordinated Pt sites [9, 24].

4.3 Effects of Pt/Zn-modified TiO_2 preparation method

From the results in part of the effects of amount of Zn, the Pt/Zn-modified TiO_2 with the optimum of Zn/Ti equals to 0.01 gave the highest VA yield. In this part, the catalyst preparation method of Pt/TiO_2-0.01Zn would further studied. The catalyst which Pt precursor was impregnated on solvothermal 0.01Zn-modified TiO_2 was referred to conv-Pt/TiO_2-0.01Zn. While the catalyst prepared by impregnation Zn precursor and Pt precursor on solvothermal TiO_2 sequentially was referred to seq-Pt/TiO_2-0.01Zn. Moreover, the Pt and Zn precursor was promptly impregnated on solvothermal TiO_2 was referred to co-Pt/TiO_2-0.01Zn.

4.3.1 Catalyst Characterization

4.3.1.1 X-ray diffraction (XRD)

The XRD patterns of Pt/TiO_2-0.01Zn prepared by conventional-impregnation method, sequential-impregnation method and co-impregnation method are shown in Figure 4.9. The anatase TiO_2 was the major phase in all of catalysts and only small fraction of rutile was observed. The crystallite size of conventional catalyst exhibited the smaller TiO_2 crystallite size than the others as shown in Table 4.7.

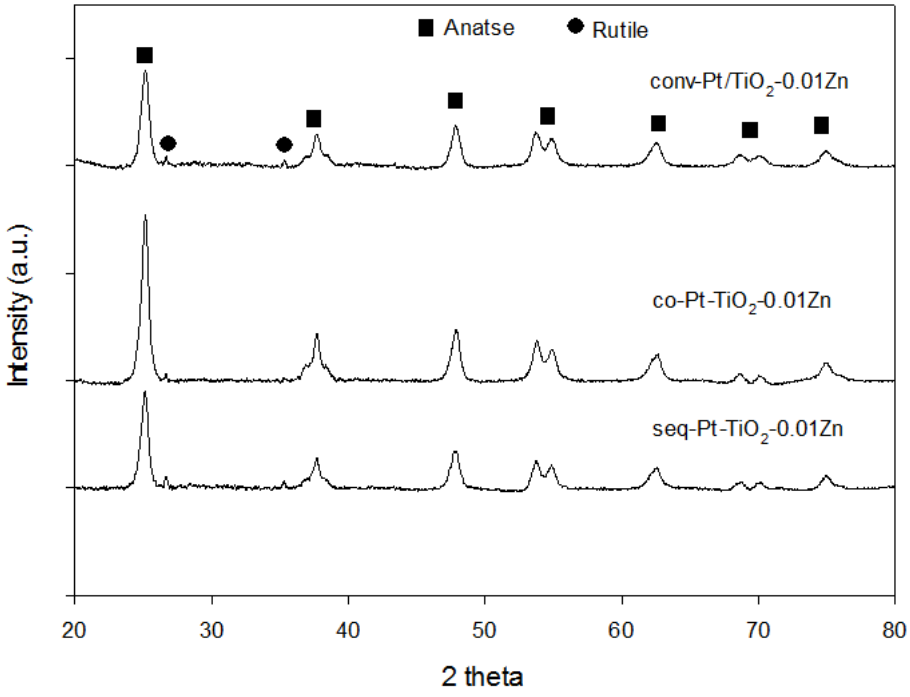

Figure 4.9 XRD patterns of Pt/TiO_2-0.01Zn catalysts prepared by different methods

4.3.1.2 N_2-physisorption

The properties of Pt/TiO_2 and Pt/TiO_2-0.01Zn prepared by different methods such as BET surface area, average pore diameter, pore volume and average TiO_2 crystallite size are shown in Table 4.7. All the modified catalysts showed the greater BET surface area than the unmodified catalyst. Therefore, adding Zn into catalyst led to the higher surface area. Among the Zn-modified catalysts, the catalysts prepared by conventional impregnation exhibited the highest surface area (98 m^2/g) compared to the other preparation methods (around 80 m^2/g). While the surface area of seq-impregnation catalysts was quite similar to the co-impregnation catalysts.

Table 4.7 Physical properties of Pt/TiO_2 and Pt/Zn-modified TiO_2 catalysts prepared by different methods

Catalyst	BET surface area (m^2/g)	Average pore diameter (nm)	Pore volume (cm^3(STP)/g)	TiO_2 Crystallite size (nm)
Pt/TiO_2	75	13.5	0.32	16.0
Pt/TiO_2-0.01Zn (conv-impregnation)	98	11.0	0.35	11.2
Pt/TiO_2-0.01Zn (seq-impregnation)	78	11.6	0.29	13.9
Pt/TiO_2-0.01Zn (co-impregnation)	80	14.3	0.36	14.5

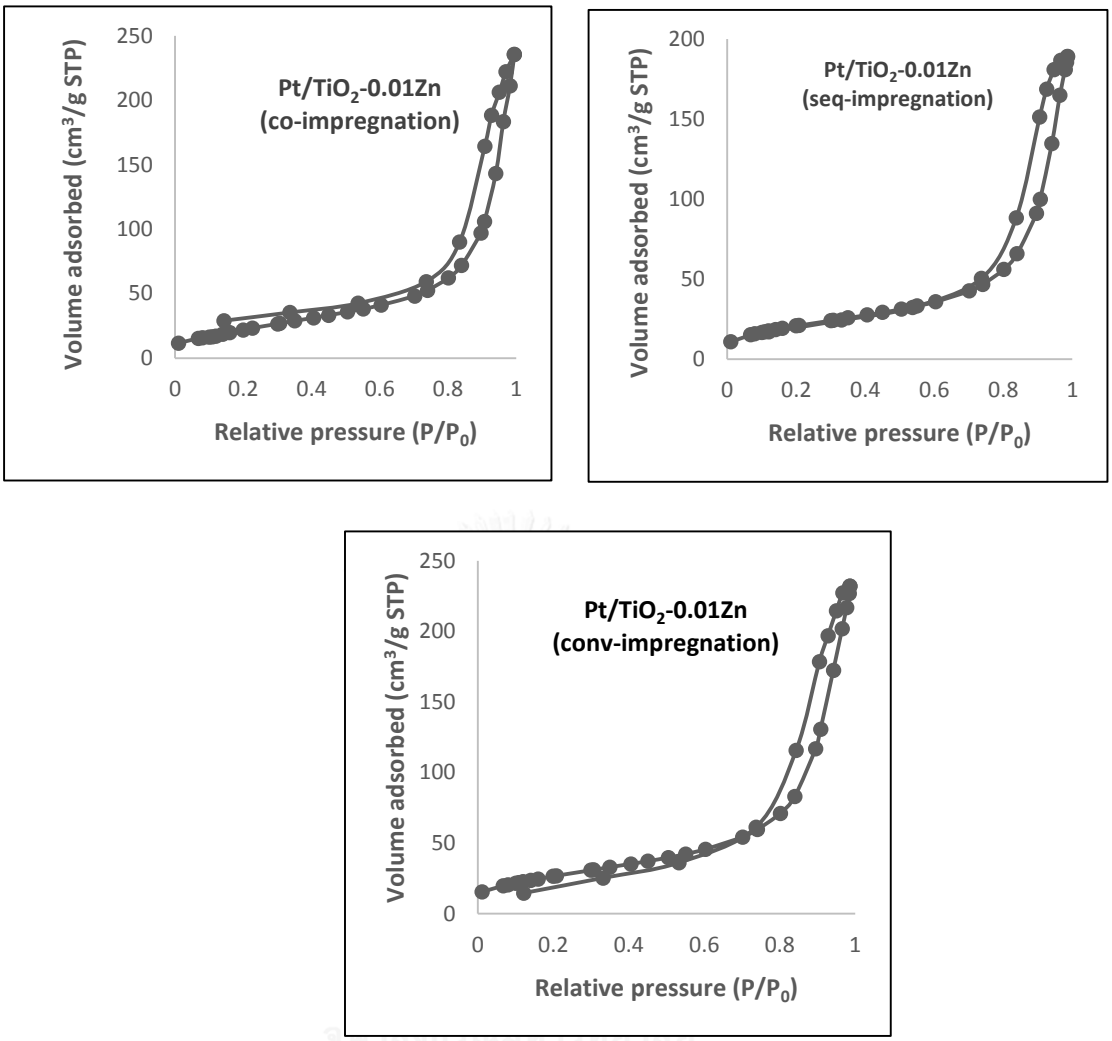

Figure 4.10 N_2 adsorption-desorption isotherms at -196 ℃ of Pt/TiO_2 -0.01Zn prepared by various methods

The Zn-modified catalyst prepared by different methods had the pore diameter in range of 11-14 nm and exhibited the mesoporous structure. The sequential-impregnation catalysts showed the lowest surface area and pore volume about 78 m^2/g and 0.29 cm^3 (STP)/g, respectively due to pore blocking by ZnO or Pt particles.

4.3.1.3 H_2-temperature programmed reduction (H_2-TPR)

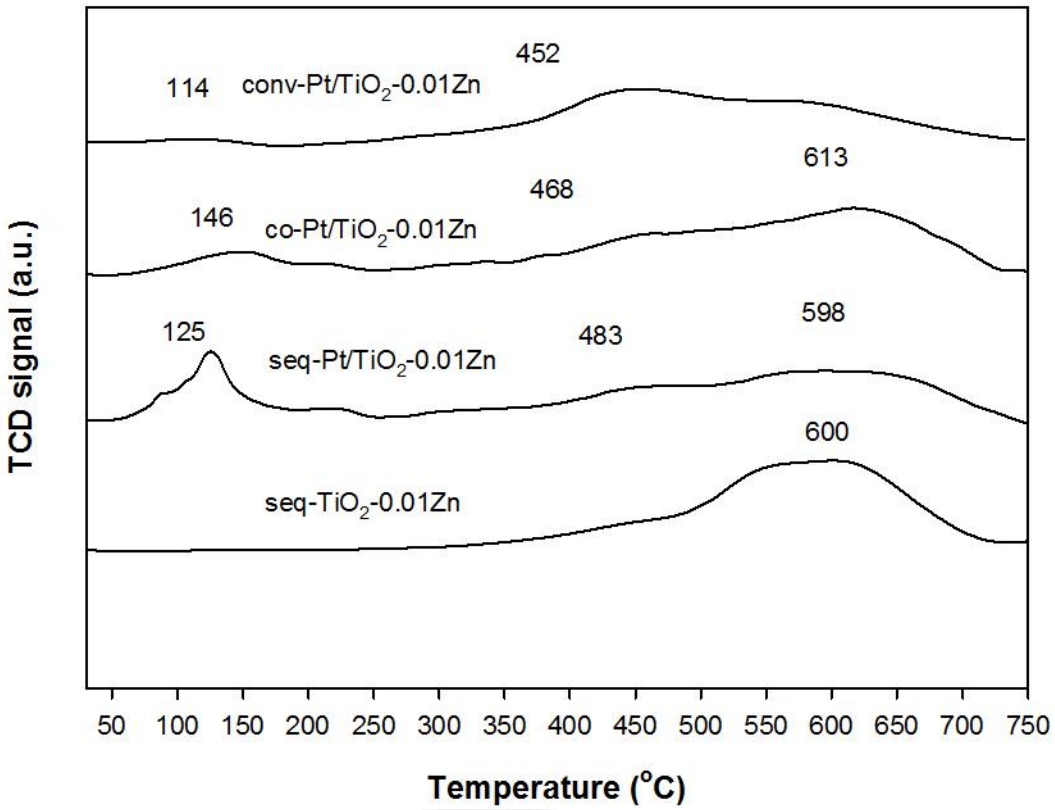

Figure 4.11 H_2-TPR profiles of TiO_2, Pt/TiO_2 and Pt/Zn-modified TiO_2

The reduction behavior of Pt/TiO_2-0.01Zn prepared by different methods were examined by H_2-TPR technique and is shown in Figure 4.11. The Pt oxide reduction peak (first peak) of Pt/TiO_2-0.01Zn prepared by seq-impregnation and co-impregnation methods were higher than the conv-impregnation. This may be due to the agglomeration of Pt particles which led to the low Pt dispersion according to CO-chemisorption results. Moreover, the sequential impregnation and co-impregnation method provided the stronger interaction between metal and support.

4.3.1.4 CO-chemisorption

The conventional impregnation catalyst showed the higher amount of active sites than the catalyst prepared by other methods at both of low and high reduction temperatures as shown in Table 4.8. The Zn-modified catalyst prepared by sequential and co-impregnation catalysts exhibited the same amount of active sites.

Table 4.8 CO-chemisorption of Pt/TiO_2 and Pt/Zn-modified TiO_2 catalysts prepared by different methods.

Catalysts	Reduction temperature (°C)	%Pt dispersion	Amount of active sites ($x10^{18}$ molecule CO/g cat)
Pt/TiO_2	200	69	10.6
	500	43	6.7
conv-Pt/TiO_2-0.01Zn	200	54	8.3
	500	53	8.2
seq-Pt/TiO_2-0.01Zn	200	39	6.0
	500	48	7.5
co-Pt/TiO_2-0.01Zn	200	39	6.0
	500	48	7.5

4.3.1.5 X-ray photoelectron spectroscopy (XPS)

XPS spectra of Ti2p and Zn2p of Pt/TiO_2-0.01Zn are shown in Figure 4.12 and Figure 4.13, respectively. Ti2p peak at 459 eV and 464.6 eV was related to $Ti_{2p3/2}$ and $Ti_{2p1/2}$, respectively which were related to Ti^{4+} species. All of Zn-modified catalysts exhibited the same position of Zn2p spectra at 1023 and 1046 eV which corresponded to Zn $2p_{3/2}$ and Zn $2p_{1/2}$. The Zn ions were in form of Zn^{2+} or ZnO dispersed on the surface of TiO_2 crystal.

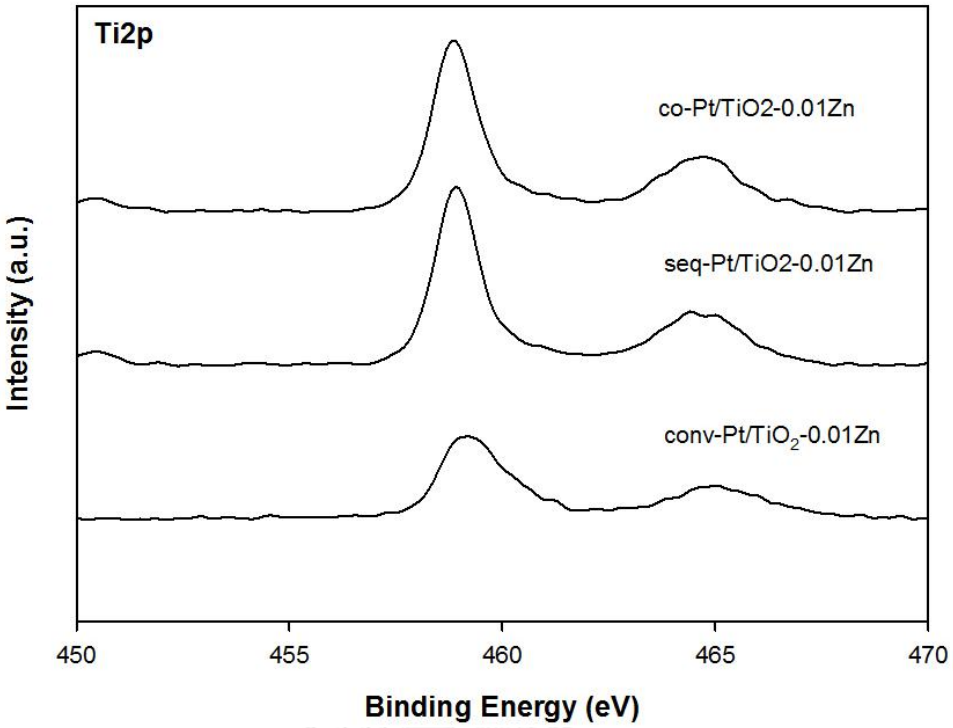

Figure 4.12 XPS spectra of Ti2p of Pt/TiO_2-0.01Zn prepared by different methods

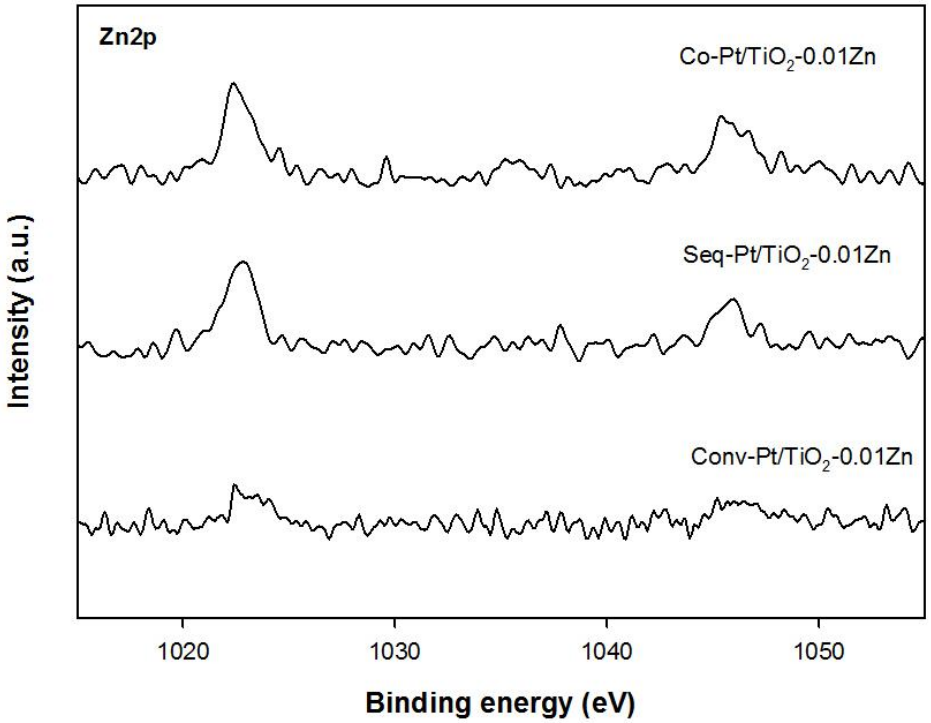

Figure 4.13 XPS spectra of Zn2p of Pt/TiO_2-0.01Zn prepared by different methods

4.3.1.6 FT-IR analysis for CO adsorbed on the catalyst (CO-IR)

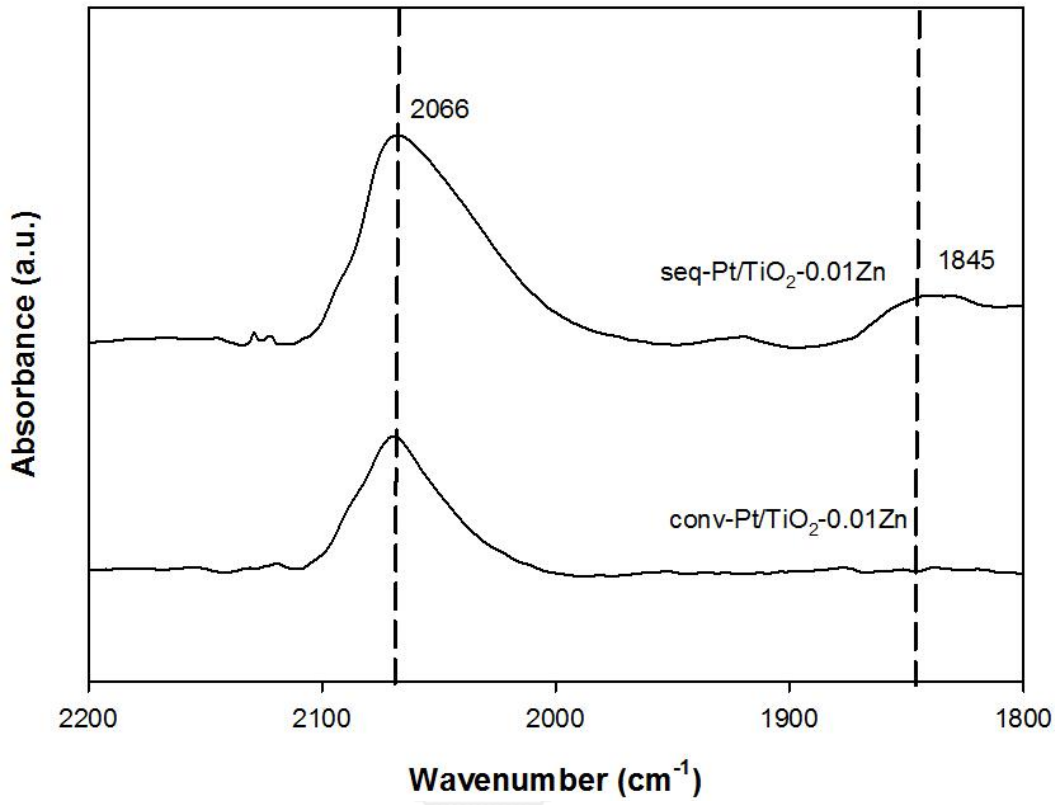

Figure 4.14 FT-IR spectra of a probe molecule of CO adsorbed on Pt/TiO_2-0.01Zn prepared by different synthesis which reduced at 200 °C

The FT-IR spectra of a probe molecule of CO adsorbed on Pt/TiO_2-0.01Zn prepared by different synthesis which reduced at 200 °C are shown in Figure 4.14. The adsorption band at 2066 cm^{-1} and 1845 cm^{-1} were related to the CO linear adsorption on Pt edge sites and bridge-type CO adsorbed[22]. For seq-impregnation, there was an appearance of bridge-type CO adsorbed over the Pt terrace sites. It has been reported that CO adsorbs in a bridge form mainly on large Pt particles, while linear adsorbed CO on small particles. According to H_2-TPR results, the Pt oxide reduction peak shifted to the higher temperature implied to the larger particles of Pt. Therefore, low VA selectivity of seq-impregnation catalysts at 48% due to less amount of low coordinated Pt sites.

4.3.2 Effects of catalyst preparation method on catalytic performances of Pt/Zn-modified TiO_2 in the liquid phase selective hydrogenation of 3-nitrostyrene

The Zn-modified catalyst with the optimum Zn/Ti molar ratio (0.01 Zn/Ti) were prepared by different methods. Prior to the reaction test, the catalysts were reduced at different temperatures at 200 °C and 500 °C. The results of catalytic performances are shown in Table 4.9. At low reduction temperature, the Pt supported on Zn-modified TiO_2 which prepared by conventional impregnation method showed higher conversion than the catalysts prepared by the other methods. According to CO chemisorption results, the catalysts prepared by conventional-impregnation method had the highest %Pt dispersion.

Table 4.9 Reaction results of Pt/TiO_2 and Pt/Zn-modified TiO_2 catalysts prepared by different methods

Catalyst	Reduction temperature (°C)	Conv (%)	VA selectivity (%)	Yield (%)	Dispersion (%)
Pt/TiO_2-0.01Zn	200	43	65	28	54
(conv-impregnation)	500	63	84	53	53
Pt/TiO_2-0.01Zn	200	37	48	18	39
(seq-impregnation)	500	55	79	43	48
Pt/TiO_2-0.01Zn	200	37	62	23	39
(co-impregnation)	500	55	79	44	48

4.4 The effects of amount of La on the properties of TiO_2 and Pt catalysts supported on La-modified TiO_2 supports

4.4.1 Catalyst Characterization

4.4.1.1 X-ray diffraction (XRD)

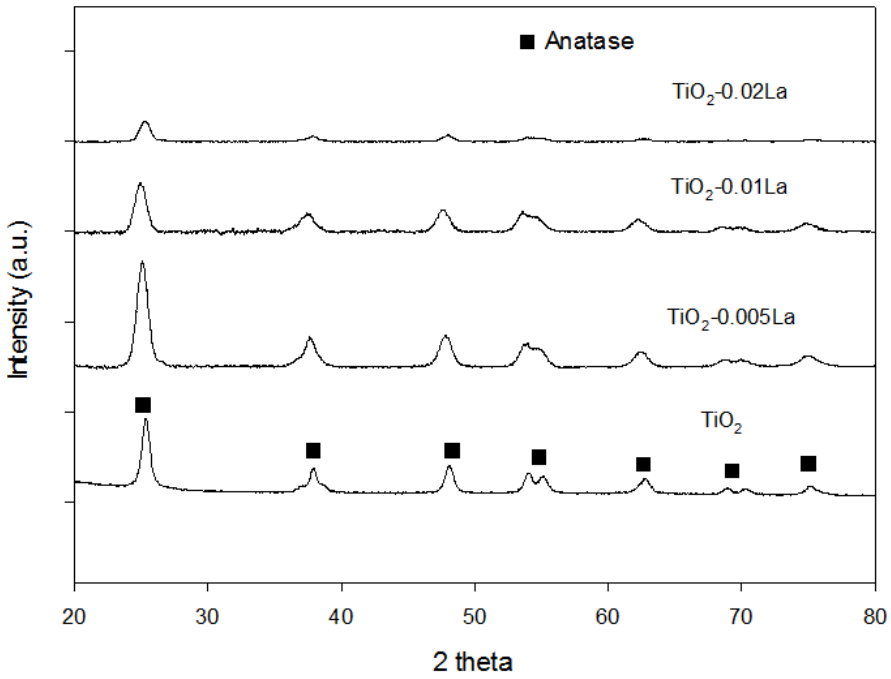

Figure 4.15 XRD patterns of TiO_2 and La-modified TiO_2

The TiO_2 and La-modified TiO_2 were prepared by solvothermal method. The X-ray diffraction was used to determine the TiO_2 phase and TiO_2 crystallite size. All of TiO_2 showed only anatase phase. The XRD patterns of TiO_2 and La-modified TiO_2 are shown in Figure 4.15. The characteristic peaks of anatase phase TiO_2 were observed at 25°(anatase major peak), 37°, 49°, 54°, 63°, 69° and 75° 2θ in all supports. All of La-modified TiO_2 had smaller crystallite size than the unmodified TiO_2. Furthermore, the crystallite size of TiO_2 tended to be smaller when the molar ratio of La/Ti were increased[52].

All of Pt/TiO_2 catalysts were prepared by incipient wetness impregnation method. The XRD patterns shows only the anatase TiO_2 phase of Pt/TiO_2 and Pt/La-modified TiO_2 with no other TiO_2 phases were observed as shown in Figure 4.16. The crystallite size of anatase phase were decreased with increasing molar ratio of La/Ti from 0.005-0.02. The characteristic peaks of Pt species were not detected due to low Pt loading (0.5%wt Pt loading) and/or good dispersion of Pt on TiO_2 support.

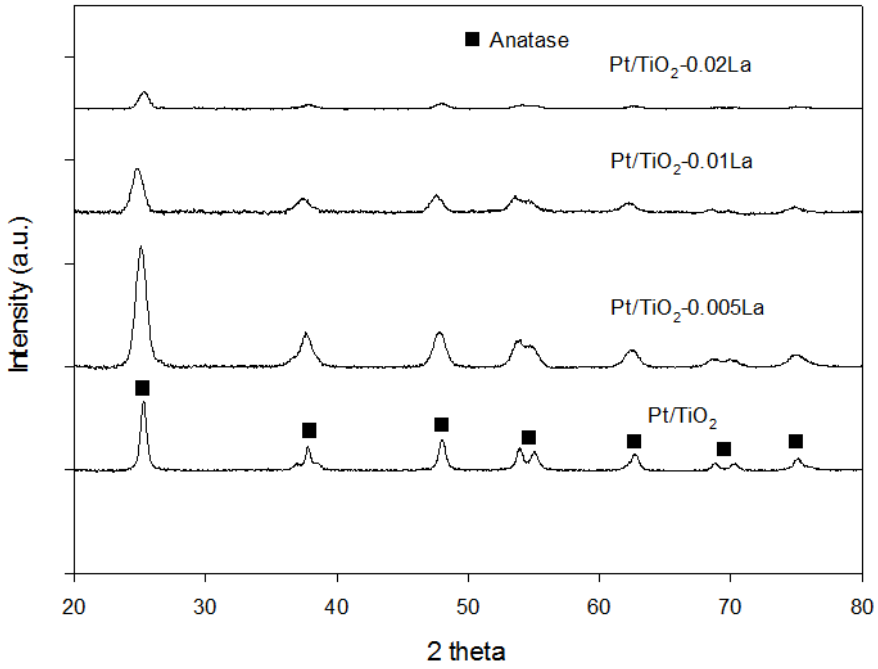

Figure 4.16 XRD patterns of Pt/TiO_2 and Pt/La-modified TiO_2 catalysts

4.4.1.2 N_2-physisorption

The BET surface area of La-modified TiO_2 were higher than the unmodified TiO_2 as shown in Table 4.10. The results clearly shows that the presence of La can increase specific surface area and restrain the growth of TiO_2 crystallites[53].

Table 4.10 Physical properties of TiO_2 and La-modified TiO_2

Support	BET surface area (m^2/g)	Average pore diameter (nm)	Pore volume (cm^3(STP)/g)	TiO_2 Crystallite size (nm)
TiO_2	83	14.5	0.38	16.5
TiO_2-0.005La	110	12.2	0.40	8.5
TiO_2-0.01La	119	12.9	0.44	7.8
TiO_2-0.02La	-	-	-	7.5

Table 4.11 Physical properties of Pt/TiO_2 and Pt/La-modified TiO_2 catalysts

Catalyst	BET surface area (m^2/g)	Average pore diameter (nm)[a]	Pore volume ($cm^3(STP)/g$)	TiO_2 Crystallite size (nm)
Pt/TiO_2	75	13.5	0.32	16.0
Pt/TiO_2-0.005La	102	11.7	0.42	8.5
Pt/TiO_2-0.01La	123	12.8	0.51	7.9
Pt/TiO_2-0.02La	155	8.8	0.39	7.5

From the N_2-physisorption results, the BET surface area of Pt/TiO_2 was 75 m^2/g and the Pt/La-modified TiO_2 exhibited higher surface area than the unmodified catalysts. The surface area of Pt/La-modified TiO_2 were increased from 102 m^2/g to 155 m^2/g when the molar ratio of La/Ti increased from 0.005-0.02. The hysteresis loop of La-modified catalysts are shown in Figure 4.17. The unmodified catalysts showed the largest pore diameter about 13.5 nm and the Pt/TiO_2-0.01La showed the highest pore volume about 0.51 m^2/g

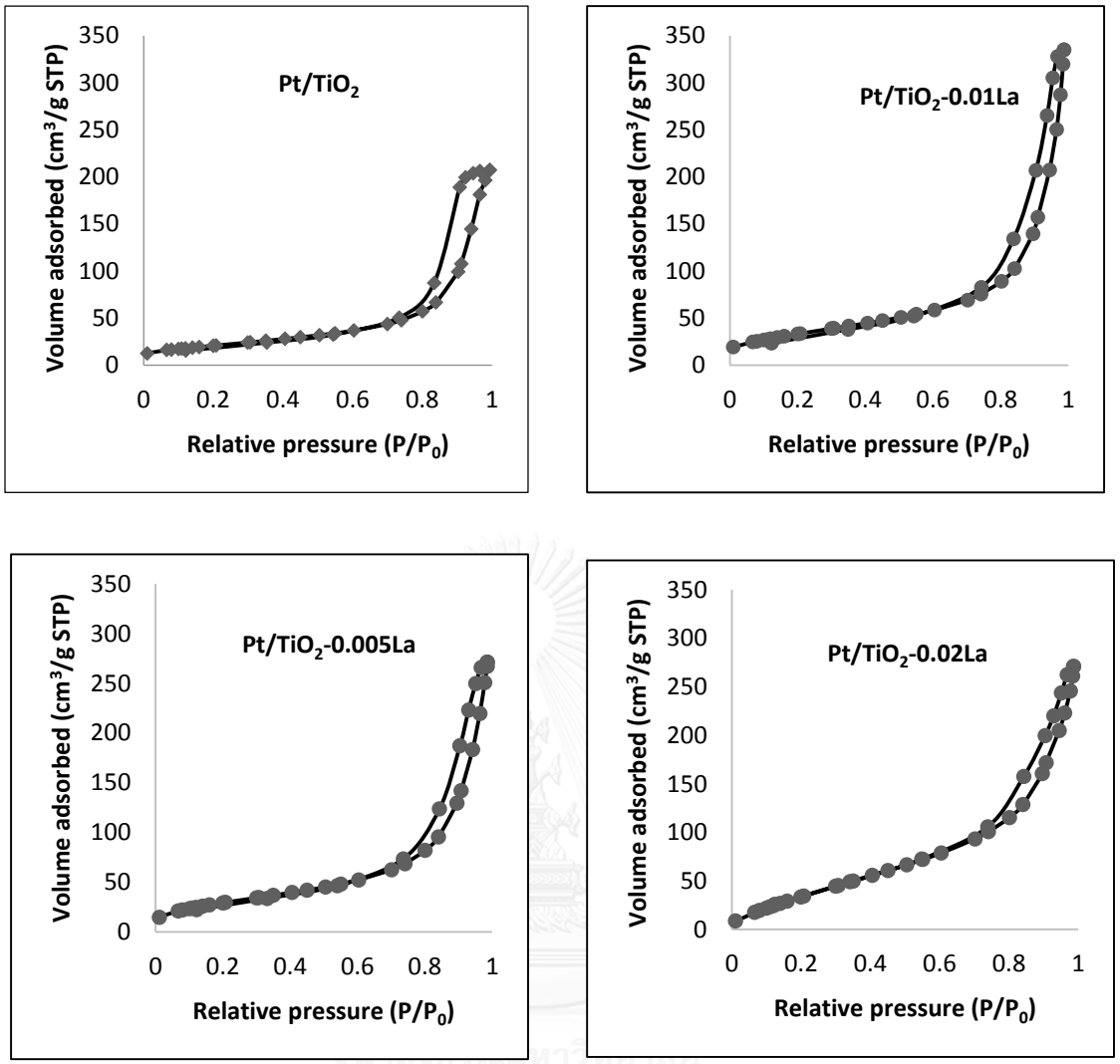

Figure 4.17 N_2 adsorption-desorption isotherms at -196 °C of Pt/TiO_2 and Pt/TiO_2-modified La at various amount of La

4.4.1.3 H_2-temperature programmed reduction (H_2-TPR)

The temperature reduction profiles were recorded for TiO_2, Pt/TiO_2 and Pt/TiO_2-modified La and are presented in Figure 4.18. The first peak was attributed to the reduction of oxidized Pt species. The first peak of Pt/TiO_2-moidifed La was shifted to the higher temperature compared to the Pt/TiO_2 which indicated that the La-modified catalysts had larger Pt particle size than the unmodified catalyst. Among the Pt/TiO_2-modified La, the Pt/TiO_2-0.01La showed the lower temperature at 109°C than the Pt/TiO_2-0.005La and Pt/TiO_2-0.02La which located at 141°C and 149°C respectively. The second peak was assigned to the the Pt-TiO_x species reduction. The higher peak shift was assigned to the stronger metal-support interaction. The peak was shifted to lower temperature when the molar ratio of La/Ti was increased indicating the weaker Pt-TiO_2 interaction of La-modified catalysts. The last peak corresponding to the reduction of capping oxygen of TiO_2.

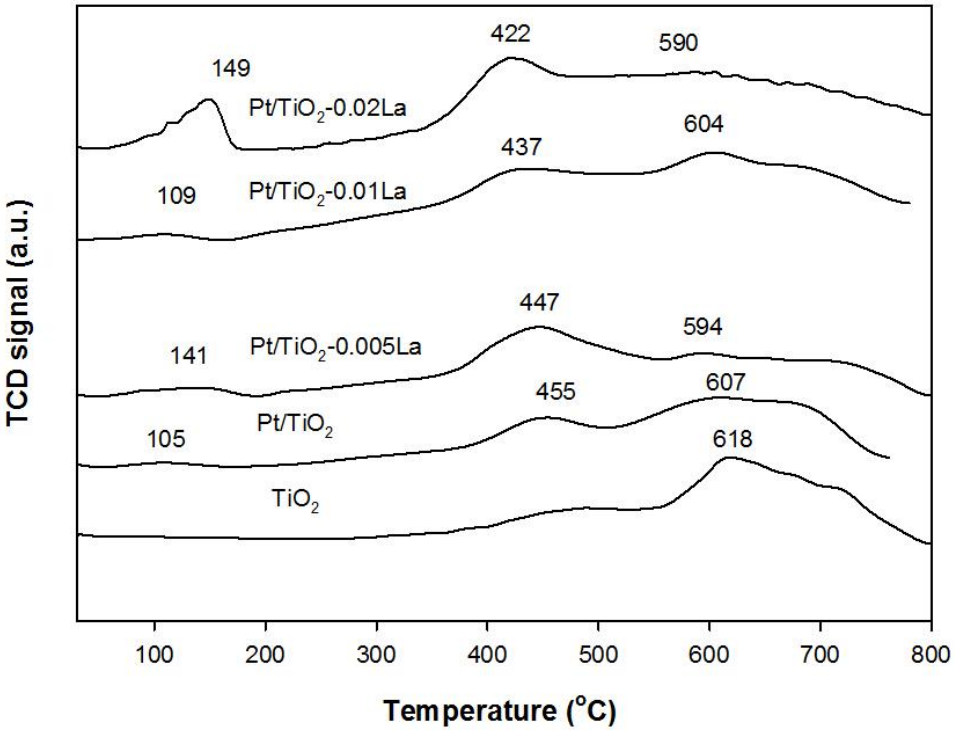

Figure 4.18 H_2-TPR profiles of Pt/TiO_2 and Pt/La-modified TiO_2

4.4.1.4 CO-chemisorption

Table 4.12 %Pt dispersion and amount of active sites of catalysts reduced at 200 °C and 500 °C.

Catalysts	Reduction temperature (°C)	%Pt dispersion	Amount of active sites (x10^{18} molecule CO/g cat)
Pt/TiO_2	200	69	10.6
	500	43	6.7
Pt/TiO_2-0.005La	200	48	7.4
	500	45	6.9
Pt/TiO_2-0.01La	200	62	9.6
	500	59	9.2
Pt/TiO_2-0.02La	200	27	4.2
	500	26	3.9

4.4.1.5 X-ray photoelectron spectroscopy (XPS)

The XPS spectra of La3d of Pt/0.02La-modified TiO_2 are shown in Figure 4.19. The signals were very weak due to low concentration of La. There were two spin orbit which related to $La3d_{5/2}$ and $La3d_{3/2}$. It can be observed that each of spin orbit were separated into double peak structures. The $La3d_{5/2}$ was located at 835.1 and 839.5 eV and the $La3d_{3/2}$ was located at 852.0 and 856.4 eV. According to Ping Zhang *et al*. [54], the energy gap between two spin orbit was about 17.1 eV and the separation between satellite and main peak was about 4.5 eV corresponding to La^{3+} compounds or in form of La_2O_3.

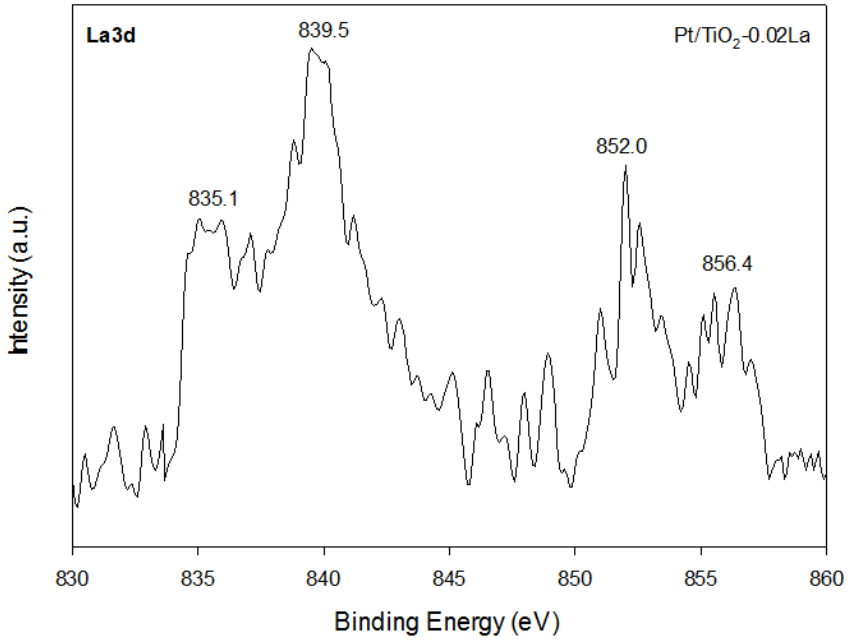

Figure 4.19 XPS spectra of La3d of Pt/TiO_2-0.02La

4.4.1.6 Transmission electron microscopy (TEM)

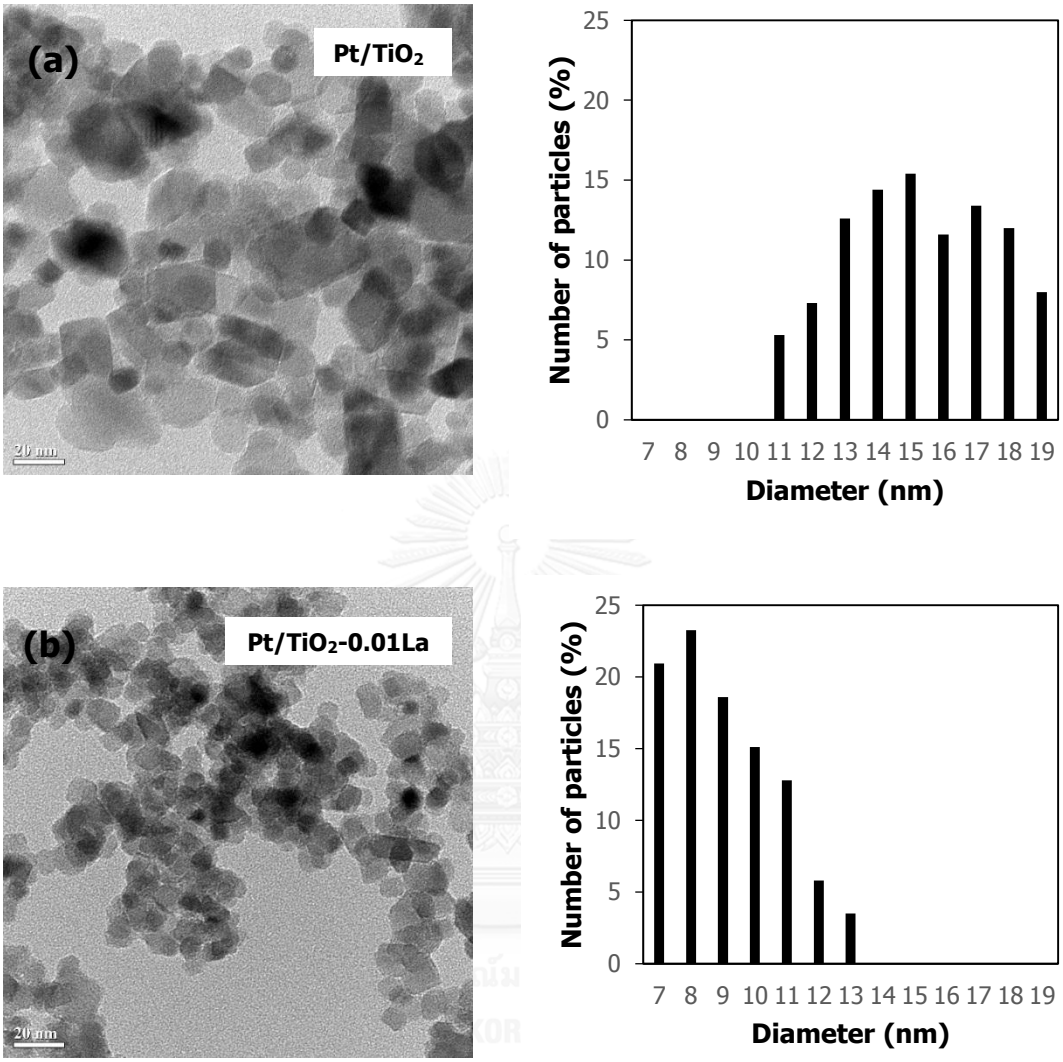

Figure 4.20 TEM images and the size distribution of (a) Pt/TiO_2 and (b) Pt/TiO_2.-0.01La

Figure 4.20 shows the TEM images and particle sizes distribution of Pt/TiO_2 and Pt/TiO_2-0.01La. The TiO_2 particle size distribution of the former was in range of 11-19 nm and 7-13 nm for the latter which were in good agreement with the XRD results. The results clearly showed that the presence of La in TiO_2 support led to the smaller of TiO_2 crystallite size. The formation of La-modified TiO_2 by solvothermal process, La^{3+} were dispersed in TiO_2 precursor and solvent. The La^{3+} ions difficultly entered to the TiO_2 lattice due to the bigger ion radius (0.115 nm) than Ti^{4+} radius (0.068 nm). Therefore, the La^{3+} possibly dispersed on the TiO_2 surface as La_2O_3 according to the

results of XPS[53]. The Pt particles cannot be detected due to small particles and/or good dispersion of Pt.

4.4.2 Catalytic performances of Pt/La-modified TiO_2 in the liquid phase selective hydrogenation of 3-nitrostyrene

The catalyst were reduced at 200 °C or 500 °C in H_2 flow before the reaction test for 60 minutes. At low reduction temperature (200 °C), the conversion of all La-modified TiO_2 were decreased in range of 49-70% compared to Pt/TiO_2 at about 80%. Moreover, the Pt/0.01La-modified catalyst showed the best conversion among the group of La-modified catalysts. According to the CO chemisorption results, the La-modified TiO_2 had lower %Pt dispersion or less amount of active sites than the unmodified catalyst. Moreover, the first peak of H_2-TPR of La modified catalyst which corresponding to Pt oxide reduction shift to higher temperature indicated the larger Pt particles or lower reducibility. At high reduction temperature (500 °C), the conversion of La-modified catalyst were decreased due to the partial coverage of Pt by La_2O_3 or/and TiO_{2-x} species [9].

Table 4.13 Reaction results of the Pt/TiO_2 catalysts and Pt/La-modified TiO_2 catalysts

Catalyst	Reduction temperature (°C)	Conv (%)	VA selectivity (%)	Yield (%)	Dispersion (%)
Pt/TiO_2	200	80	77	61	69
	500	44	86	38	43
Pt/TiO_2-0.005La	200	51	66	34	48
	500	41	79	33	45
Pt/TiO_2-0.01La	200	70	74	51	62
	500	56	88	49	59
Pt/TiO_2-0.02La	200	49	46	23	27
	500	24	62	15	26

4.5 Comparison between Pt/Zn-modified TiO_2 and Pt/La-modified TiO_2

The comparison between the Zn-modified catalyst and La-modified catalyst would be discussed in this part. At the high reduction temperature and the same ratio of Zn/Ti and La/Ti, the Zn-modified catalyst showed the higher conversion than the La-modified catalyst. As mentioned in the previous part, the Pt active sites of Pt/La-modified TiO_2 were partially covered by the La_2O_3 or/and TiO_{2-x} species affected the lower conversion than the low reduction temperature. While the Zn-modified catalyst exhibited the higher conversion than the unmodified catalyst and La-modified catalyst because the Pt-Zn strong interaction or PtZn alloy that the electron from Zn was shifted to Pt.

Table 4.14 Reaction results of the Pt/TiO_2 catalysts, Pt/Zn-modified TiO_2 catalysts and Pt/La-modified TiO_2 catalysts

Catalyst	Reduction temperature (°C)	Conv (%)	VA selectivity (%)	Yield (%)	Dispersion (%)
Pt/TiO_2	200	80	77	61	69
	500	44	86	38	43
Pt/TiO_2-0.005Zn	200	79	80	63	55
	500	64	80	51	58
Pt/TiO_2-0.01Zn	200	43	65	28	54
	500	63	84	53	53
Pt/TiO_2-0.02Zn	200	26	68	18	37
	500	54	75	41	51
Pt/TiO_2-0.005La	200	51	66	34	48
	500	41	79	33	45
Pt/TiO_2-0.01La	200	70	74	51	62
	500	56	88	49	59
Pt/TiO_2-0.02La	200	49	46	23	27
	500	24	62	15	26

CHAPTER V
CONCLUSIONS AND RECOMMENDATIONS

The effects of the amount of Zn and La modified TiO_2 were investigated in the liquid phase selective hydrogenation of 3-nitrostyrene. Moreover, the effects of catalysts preparation of the optimum ratio of Zn/Ti of Zn-modified catalyst was also studied. The conclusions and the recommendations are shown below.

Conclusions

Based on the CO-chemisorption results, the Zn-modified catalysts exhibited lower dispersion than the unmodified catalysts at low reduction temperature due to the dilution of Pt surfaces by Zn. In contrast, at high reduction temperatures, the Zn-modified catalysts showed higher dispersion which led to the higher conversion than the unmodified catalysts. Moreover, the strong Pt-Zn interaction at high reduction temperatures provided the electron transfer from Zn to Pt which improved the conversion. The CO-IR spectra of the unmodified catalyst and Zn-modified catalyst exhibited only the linear CO adsorption on low coordinated Pt sites which facilitated high VA selectivity.

The addition of La on TiO_2 supports provided smaller crystallite size and higher surface area. However, all of the La-modified catalysts gave less amount of active sites compared to the unmodified catalysts, resulting in the lower conversion of 3-nitrostyrene.

Recommendations

1) The presence of PtZn alloy in Pt/Zn-modofied TiO_2 should further analysis by the other techniques.
2) The study of the stability of Zn-modified catalyst and La-modified catalyst compared to the unmodified catalyst should be investigated.

REFERENCES

[1] Serna, P. and Corma, A. Transforming Nano Metal Nonselective Particulates into Chemoselective Catalysts for Hydrogenation of Substituted Nitrobenzenes. ACS Catalysis 5(12) (2015): 7114-7121.

[2] Dey, J., Saha, M., Pal, A.K., and Ismail, K. Regioselective nitration of aromatic compounds in an aqueous sodium dodecylsulfate and nitric acid medium. RSC Advances 3(40) (2013): 18609-18613.

[3] Luo, P., et al. Highly efficient and selective reduction of nitroarenes with hydrazine over supported rhodium nanoparticles. Catalysis Science & Technology 2(2) (2012): 301-304.

[4] Yarulin, A., Berguerand, C., Yuranov, I., Cárdenas-Lizana, F., Prokopyeva, I., and Kiwi-Minsker, L. Pt–Zn nanoparticles supported on porous polymeric matrix for selective 3-nitrostyrene hydrogenation. Journal of Catalysis 321 (2015): 7-12.

[5] Stratakis, M. and Garcia, H. Catalysis by Supported Gold Nanoparticles: Beyond Aerobic Oxidative Processes. Chemical Reviews 112(8) (2012): 4469-4506.

[6] Yarulin, A., Berguerand, C., Alonso, A.O., Yuranov, I., and Kiwi-Minsker, L. Increasing Pt selectivity to vinylaniline by alloying with Zn via reactive metal–support interaction. Catalysis Today 256, Part 2 (2015): 241-249.

[7] Xu, G., Wei, H., Ren, Y., Yin, J., Wang, A., and Zhang, T. Chemoselective hydrogenation of 3-nitrostyrene over a Pt/FeOxpseudo-single-atom-catalyst in CO2-expanded liquids. Green Chem. 18(5) (2016): 1332-1338.

[8] Bailón-García, E., Carrasco-Marín, F., Pérez-Cadenas, A.F., and Maldonado-Hódar, F.J. Selective hydrogenation of citral by noble metals supported on carbon xerogels: Catalytic performance and stability. Applied Catalysis A: General 512 (2016): 63-73.

[9] Corma, A., Serna, P., Concepcion, P., and Calvino, J.J. Transforming nonselective into chemoselective metal catalysts for the hydrogenation of substituted nitroaromatics. J Am Chem Soc 130(27) (2008): 8748-53.

[10] Chen, C.-S., You, J.-H., Lin, J.-H., and Chen, Y.-Y. Effect of highly dispersed active sites of Cu/TiO2 catalyst on CO oxidation. Catalysis Communications 9(14) (2008): 2381-2385.

[11] Comsup, N., Panpranot, J., and Praserthdam, P. The influence of Si-modified TiO2 on the activity of Ag/TiO2 in CO oxidation. Journal of Industrial and Engineering Chemistry 16(5) (2010): 703-707.

[12] Abazović, N.D., et al. Synthesis and Characterization of Rutile TiO(2)Nanopowders Doped with Iron Ions. Nanoscale Research Letters 4(6) (2009): 518-525.

[13] Tauster, S.J., Fung, S.C., and Garten, R.L. Strong metal-support interactions. Group 8 noble metals supported on titanium dioxide. Journal of the American Chemical Society 100(1) (1978): 170-175.

[14] Vannice, M.A. and Poondi, D. Benzaldehyde Hydrogenation over Titania-Covered Pt Powder. Journal of Catalysis 178(1) (1998): 386-390.

[15] Bagheri, S., Muhd Julkapli, N., and Bee Abd Hamid, S. Titanium dioxide as a catalyst support in heterogeneous catalysis. ScientificWorldJournal 2014 (2014): 727496.

[16] Ananthan, S.A. and Narayanan, V. TiO<inf>2</inf> supported Ru and Pt nano catalysts for selective hydrogenation of citral. in Green Technology and Environmental Conservation (GTEC 2011), 2011 International Conference on, pp. 5-11, 2011.

[17] Yoshida, H., Igarashi, N., Fujita, S.-i., Panpranot, J., and Arai, M. Influence of Crystallite Size of TiO2 Supports on the Activity of Dispersed Pt Catalysts in Liquid-Phase Selective Hydrogenation of 3-Nitrostyrene, Nitrobenzene, and Styrene. Catalysis Letters 145(2) (2014): 606-611.

[18] Boronat, M., Concepción, P., Corma, A., González, S., Illas, F., and Serna, P. A Molecular Mechanism for the Chemoselective Hydrogenation of Substituted Nitroaromatics with Nanoparticles of Gold on TiO2 Catalysts: A Cooperative Effect between Gold and the Support. Journal of the American Chemical Society 129(51) (2007): 16230-16237.

[19] Shimizu, K.-i., Miyamoto, Y., Kawasaki, T., Tanji, T., Tai, Y., and Satsuma, A. Chemoselective Hydrogenation of Nitroaromatics by Supported Gold Catalysts: Mechanistic Reasons of Size- and Support-Dependent Activity and Selectivity. The Journal of Physical Chemistry C 113(41) (2009): 17803-17810.

[20] Serna, P., Concepción, P., and Corma, A. Design of highly active and chemoselective bimetallic gold–platinum hydrogenation catalysts through kinetic and isotopic studies. Journal of Catalysis 265(1) (2009): 19-25.

[21] Yoshida, H., et al. Hydrogenation of Nitrostyrene with a Pt/TiO2 Catalyst in CO2-Dissolved Expanded Polar and Nonpolar Organic Liquids: Their Macroscopic and Microscopic Features. The Journal of Physical Chemistry C 115(5) (2011): 2257-2267.

[22] Fujita, S.-i., Yoshida, H., Asai, K., Meng, X., and Arai, M. Selective hydrogenation of nitrostyrene to aminostyrene over Pt/TiO2 catalysts: Effects of pressurized carbon dioxide and catalyst preparation conditions. The Journal of Supercritical Fluids 60 (2011): 106-112.

[23] Beier, M.J., Andanson, J.-M., and Baiker, A. Tuning the Chemoselective Hydrogenation of Nitrostyrenes Catalyzed by Ionic Liquid-Supported Platinum Nanoparticles. ACS Catalysis 2(12) (2012): 2587-2595.

[24] Pisduangdaw, S., Mekasuwandumrong, O., Yoshida, H., Fujita, S.-I., Arai, M., and Panpranot, J. Flame-made Pt/TiO2 catalysts for the liquid-phase selective hydrogenation of 3-nitrostyrene. Applied Catalysis A: General 490 (2015): 193-200.

[25] Tjong, S.C. Nanocrystalline Materials : Their Synthesis-Structure-Property Relationships and Applications. ELSEVIER, 2006.

[26] Lai, J., Niu, W., Luque, R., and Xu, G. Solvothermal synthesis of metal nanocrystals and their applications. Nano Today 10(2) (2015): 240-267.

[27] Nam, W.S. and Han, G.Y. Characterization and Photocatalytic Performance of Nanosize TiO 2 Powders Prepared by the Solvothermal Method. Korean Journal of Chemical Engineering 20(6) (2003): 1149-1153.

[28] Asim, N., Ahmadi, S., Alghoul, M.A., Hammadi, F.Y., Saeedfar, K., and Sopian, K. Research and Development Aspects on Chemical Preparation Techniques of

Photoanodes for Dye Sensitized Solar Cells. International Journal of Photoenergy 2014 (2014): 21.

[29] Kim, C.-S., Moon, B.K., Park, J.-H., Choi, B.-C., and Seo, H.-J. Solvothermal synthesis of nanocrystalline TiO2 in toluene with surfactant. Journal of Crystal Growth 257(3–4) (2003): 309-315.

[30] platinum(Pt). (2012).

[31] Platinum Available from: https://en.wikipedia.org/wiki/Platinum

[32] Zinc Available from: https://en.wikipedia.org/wiki/Zinc

[33] Bidaoui, M., et al. Toward the improvement in unsaturated alcohol selectivity during α,β-unsaturated aldehyde selective hydrogenation, using Zn as promoter of Pt. Journal of Molecular Catalysis A: Chemical 399 (2015): 97-105.

[34] Lanthanum Available from: https://en.wikipedia.org/wiki/Lanthanum

[35] Chen, X.-M., Liu, Z.-J., Tang, J.-T., Teng, C.-L., Cai, T.-J., and Deng, Q. La-modified mesoporous TiO2 nanoparticles with enhanced photocatalytic activity for elimination of VOCs. Journal of Porous Materials 22(2) (2014): 361-367.

[36] TiO2 Supported Pt Based Bimetallic Nanocatalysts for Selective Hydrogenation of Citral. Chemical Science Transactions 2(S1) (2013).

[37] Bahrig, L., Hickey, S.G., and Eychmuller, A. Mesocrystalline materials and the involvement of oriented attachment - a review. CrystEngComm 16(40) (2014): 9408-9424.

[38] Somorjai, G.A. and Carrazza, J. Structure sensitivity of catalytic reactions. Industrial & Engineering Chemistry Fundamentals 25(1) (1986): 63-69.

[39] Rioux, R.M. The Synthesis, Characterization and Catalytic Reaction Studies of Monodisperse Platinum Nanoparticles in Mesoporous Oxide Materials. Chemistry UNIVERSITY OF CALIFORNIA, BERKELEY, 2006.

[40] Sarkany, J. and D. Gonzalez, R. Support and dispersion effects on silica- and alumina-supported platinum catalysts: II. Effect on the CO-O2 reaction. Applied Catalysis 5(1) (1983): 85-97.

[41] Payakgul, W., Mekasuwandumrong, O., Pavarajarn, V., and Praserthdam, P. Effects of reaction medium on the synthesis of TiO2 nanocrystals by thermal

decomposition of titanium (IV) n-butoxide. Ceramics International 31(3) (2005): 391-397.

[42] Weerachawanasak, P., Praserthdam, P., Arai, M., and Panpranot, J. A comparative study of strong metal–support interaction and catalytic behavior of Pd catalysts supported on micron- and nano-sized TiO2 in liquid-phase selective hydrogenation of phenylacetylene. Journal of Molecular Catalysis A: Chemical 279(1) (2008): 133-139.

[43] Aware, D.V. and Jadhav, S.S. Synthesis, characterization and photocatalytic applications of Zn-doped TiO2 nanoparticles by sol–gel method. Applied Nanoscience (2015): 1-8.

[44] Pongthawornsakun, B., Mekasuwandumrong, O., Prakash, S., Ehret, E., Santos Aires, F.J.C., and Panpranot, J. Effect of reduction temperature on the characteristics and catalytic properties of TiO2 supported AuPd alloy particles prepared by one-step flame spray pyrolysis in the selective hydrogenation of 1-heptyne. Applied Catalysis A: General 506 (2015): 278-287.

[45] Silvestre-Albero, J., Sepúlveda-Escribano, A., Rodríguez-Reinoso, F., and Anderson, J.A. Influence of Zn on the characteristics and catalytic behavior of TiO2-supported Pt catalysts. Journal of Catalysis 223(1) (2004): 179-190.

[46] Fu, R., et al. Effect of different processes and Ti/Zn molar ratios on the structure, morphology, and enhanced photoelectrochemical and photocatalytic performance of Ti3+ self-doped titanium–zinc hybrid oxides. Journal of Power Sources 285 (2015): 449-459.

[47] Fu, Z., Zhang, J., Yang, X., and Cao, W. Preparation of nano-crystal N-Zn/TiO2 anode films and the effects of co-sensitization on the performance of dye-sensitized solar cells. Chinese Science Bulletin 56(19) (2011): 2001-2008.

[48] Yu, Y., Wang, J., Li, W., Zheng, W., and Cao, Y. Doping mechanism of Zn2+ ions in Zn-doped TiO2 prepared by a sol-gel method. CrystEngComm 17(27) (2015): 5074-5080.

[49] Zou, J.-J., Zhu, B., Wang, L., Zhang, X., and Mi, Z. Zn- and La-modified TiO2 photocatalysts for the isomerization of norbornadiene to quadricyclane. Journal of Molecular Catalysis A: Chemical 286(1–2) (2008): 63-69.

[50] Yarulin, A., Berguerand, C., Alonso, A.O., Yuranov, I., and Kiwi-Minsker, L. Increasing Pt selectivity to vinylaniline by alloying with Zn via reactive metal-support interaction. Catalysis Today 256 (2015): 241-249.

[51] Pisduangdaw, S., Mekasuwandumrong, O., Fujita, S.-I., Arai, M., Yoshida, H., and Panpranot, J. One step synthesis of Pt–Co/TiO2 catalysts by flame spray pyrolysis for the hydrogenation of 3-nitrostyrene. Catalysis Communications 61 (2015): 11-15.

[52] Chen, X.-M., Liu, Z.-J., Tang, J.-T., Teng, C.-L., Cai, T.-J., and Deng, Q. La-modified mesoporous TiO2 nanoparticles with enhanced photocatalytic activity for elimination of VOCs. Journal of Porous Materials 22(2) (2015): 361-367.

[53] Zhang, Y., et al. Surface phase of TiO2 modified with La2O3 and its effect on the photocatalytic H2 evolution. Materials Research Bulletin 53 (2014): 107-115.

[54] Zhang, P., Guo, J., Zhao, P., Zhu, B., Huang, W., and Zhang, S. Promoting effects of lanthanum on the catalytic activity of Au/TiO2nanotubes for CO oxidation. RSC Adv. 5(16) (2015): 11989-11995.

APPENDIX

Appendix A

CALCULATION FOR ZN-MODIFIED TiO_2 AND La-MODIFIED TiO_2 PREPARATION

Modification for TiO_2 support with various Zn/Ti and La/Ti molar ratios were prepared by solvothermal method.

Reagents:

Titanium n-butoxide = 25 g

1,4 butanediol = 100 cm^3

Zinc acetylacetonate

Lanthanum (III) nitrate hexahydrate

Example calculation: TiO_2- 0.005Zn

Weight of Titanium n-butoxide = 25 g

Molecular weight of Titanium n-butoxide = 340.35 g/mol

Mole of Titanum n-butoxide = 25 g / 340.35 g/mol = 0.0735 mol

Mole of Ti : Mole of Titanium n-butoxide = 1:1

So that mole of Ti = 0.0735 mol

Mole of Zn : Ti = 0.005 : 1

So that mole of Zn = 0.0735 * 0.005 = 0.0003675 mol

Molecular weight of Zn acetylacetonate = 263.59 g/mol

Weight of Zn acetylacetonate required = 0.0003675*263.59 = 0.0969 g

Appendix B

CALCULATION OF Pt CATALYSTS SUPPORTED ON TiO_2 AND MODIFIED TiO_2

Pt catalysts supported on TiO_2 and modified TiO_2 were prepared by incipient wetness impregnation method.

Reagent: Chloroplatinic acid (Molecular weight) = 517.90 g/mol

Support : TiO_2

Zn-modified TiO_2

La-modified TiO_2

Example of calculation: 0.5 wt.% Pt/TiO_2

Based on 1 g of catalysts used, the composition of catalysts will be as follows :

Platinum = 0.5/100 =0.005 g

TiO_2 or modified TiO_2 = 1-0.005 = 0.995 g

Platinum 0.005 g was prepared by using $H_2PtCl_6 \cdot 6H_2O$

$$= \frac{\text{MW. of } H_2PtCl_6 \cdot 6H_2O \times \text{weight of platinum required}}{\text{MW. of platinum}}$$

= (517.90 g/mol * 0.005g)/195.078 g/mol

= 0.0132 g

Chloroplatinic acid hydrate were dissolved into DI water and dropped into TiO_2, Zn and La-modified TiO_2 equal to pore volume of support to obtain 0.5% wt Pt loading.

Appendix C

CALCULATION FOR THE TiO_2 ANATASE CRYSTALLITE SIZE BY SCHERRER EQUATION

The average crystallite size of TiO_2 anatase was calculated by the half-height width of diffraction peak from XRD pattern by using the Scherrer equation:

$$D = \frac{K\lambda}{\beta cos\theta}$$

Where **D** : Crystallite size, Å

K : Shape factor of the Sherrer constant = 0.9

λ : Wavelength of the x-ray , 1.5418 Å for CuK_{α}

β : The full width-half max (FHWM) of the peak after correcting for peak broadening, which is caused by the diffractometer, radian

θ : Bragg angle , radian

The full width-half max (FHWM) of the peak after correcting for peak broadening (β) can br obtained by using Warren's equation:

$$\beta^2 = \beta_M^2 - \beta_S^2$$

So that

$$\beta = \sqrt{\beta_M^2 - \beta_S^2}$$

Where β_S: The corresponding width of standard material

β_M: The measured peak width in radians at half peak height

Example of TiO_2 crystallite size calculation: Pt/TiO_2

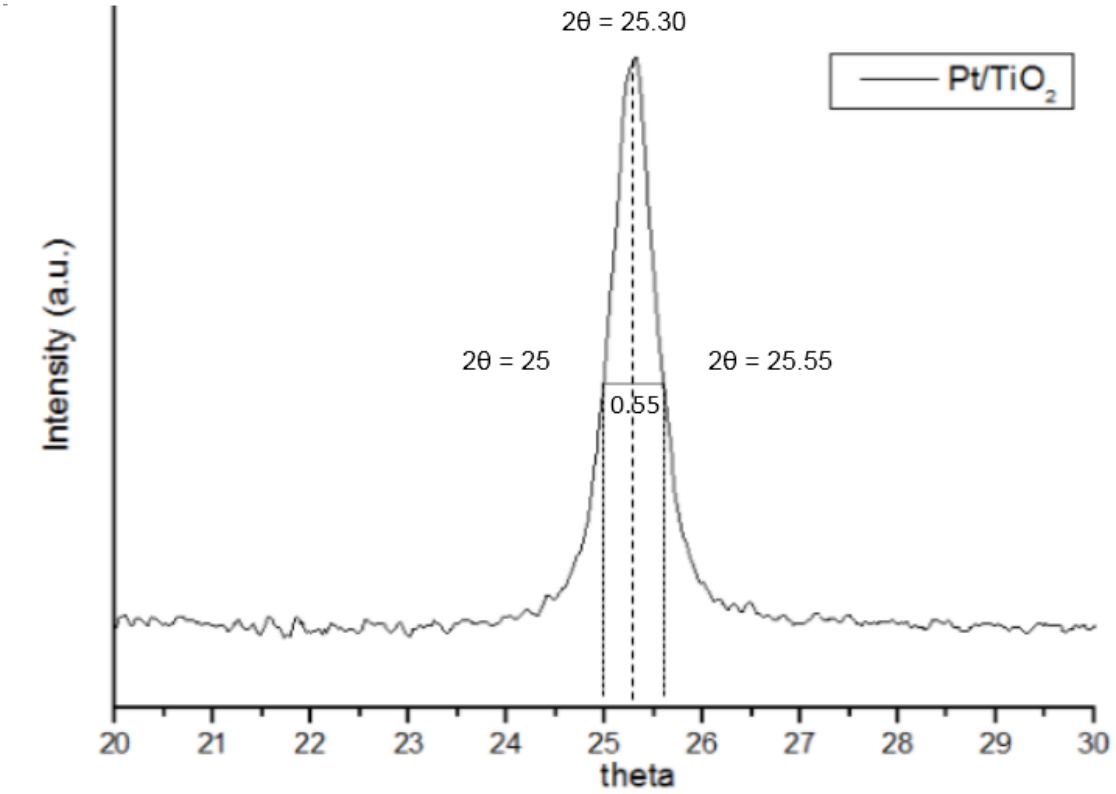

Data from graph

- Peak center of TiO_2 anatase 101: 2θ = 25.30

  θ = 12.65

- FHWM = 0.55°

  = $(2\pi * 0.55)/360$

  = 0.0096 radian

- β_M = 0.0096 radian
- β_S = 0.0041 radian

- $\beta = \sqrt{\beta_M^2 - \beta_S^2}$

  $\beta = \sqrt{0.0096^2 - 0.0041^2}$

  $\beta = 0.0087$ radian

  From Scherrer equation:

$$D = \frac{K\lambda}{\beta cos\theta}$$

$$D = \frac{0.9 \times 1.5418}{0.0087 \times cos12.65}$$

$D = 161$ Å or 16.1 nm

APPENDIX D

CALCULATION FOR METAL ACTIVE SITES AND DISPERSION

Calculation of the metal active sites and metal dispersion of the catalyst measured by CO adsorption is as follows:

Calculation of metal active sites

Let the weight of catalyst used = W g

Integral area of CO peak after adsorption = A unit

Integral area of 20 μl of standard CO peak = B unit

Amounts of CO adsorbed on catalyst = B-A unit

Volume of CO adsorbed on catalyst = 100× [(B-A)/B]

Volume of 1 mole of CO at 30°C = 24.86×10^6

Mole of CO adsorbed on catalyst = $[(B-A)/B]\ [20/24.86 \times 10^6]$ mole

Molecule of CO adsorbed on catalyst = $[20/24.86 \times 10^6]\ [6.02 \times 10^{23}]\ [(B-A)/B]$ molecules

Metal active sites = $[20/24.86 \times 10^6]\ [6.02 \times 10^{23}]\ [(B-A)/B]\ [1/W]$ molecules of CO/g of catalyst

Calculation of %metal dispersion

Definition of % metal dispersion:

$$\text{Metal dispersion (\%)} = 100 \times \frac{\text{molecules of Pt from CO adsorption}}{\text{molecules of Pt loaded}}$$

In this study, the formula from Chemisorb 2750 Operator's Manual can used for determined the % metal dispersion as follow:

$$\%D = S_f \times \frac{V_{ads}}{V_g} \times \frac{Mw}{\%M} \times 100\% \times 100\% \quad \text{.....(1)}$$

Where

%D = %metal dispersion

Sf = stoichiometry factor, (CO on Pt* =1)

Vads = volume adsorbed (cm3/g)

Vg = molar volume of gas at STP = 22414 (cm3/mol)

Mw = molecular weight of the metal (a.m.u.)

%M = %metal loading

Example: %Dispersion of 0.5%Pt/TiO_2

- Calculation Volume Chemisorbed (Vads)

$$V_{ads}(cm^3) = \frac{V_{inj}}{m} \times \sum_{i=1}^{n}(1 - \frac{A_i}{A_f}) \quad \text{.....(2)}$$

Where:

Vinj = volume injected (cm^3) = 0.020 cm^3

m = mass of sample (g)

A_i = area of peak i

A_f = area of last peak

VITA

Mr.Arnut Saeaung was born on 19 March 1992, in Bangkok, Thailand. He graduated with a Bachelor's degree in Chemical Technology from Chulalongkorn University, Thailand in 2014. He has been studying with a Master degree in Chemical Engineering from Chulalongkorn University since 2014.

List of publication :

Arnut Saeaung and Joongjai Panpranot, "Characteristics and catalytic properties of Pt/Zn-modified TiO2 in the liquid-phase selective hydrogenation of 3-nitrostyrene", Proceeding of the Pure and Applied Chemistry International Conference 2016 (PACCON 2016), Bangkok , Thailand, February 9-11, 2016.